To the Graduate Council:

I am submitting herewith a thesis written by Barbara A. Olsen entitled "Petrogenesis of the Concord Gabbro-Syenite Complex, Cabarrus County, North Carolina." I have examined the final copy of this thesis for form and content and recommend that it be accepted in partial fulfillment of the requirements for the degree of Master of Science, with a major in Geology.

Harry Y. McSween, Major Professor

We have read this thesis and recommend its acceptance:

Laurence A. Taylor

Kula C. Misra

Accepted for the Council:

Vice Chancellor
Graduate Studies and Research

PETROGENESIS OF THE CONCORD GABBRO-SYENITE COMPLEX, CABARRUS COUNTY, NORTH CAROLINA

A Thesis

Presented for the

Master of Science

Degree

The University of Tennessee, Knoxville

Barbara A. Olsen

March 1982

3058006

ACKNOWLEDGMENTS

It is a pleasure to express my thanks to those people who have lent support to this thesis. I especially thank Dr. H. Y. McSween, my thesis advisor, for first introducing me to the study area, and then providing advice, financial support and unending enthusiasm throughout the entire project. I am grateful to my committee members: Dr. L. A. Taylor, for his guidance in the use of the electron microprobe and his critical review of the text; and Dr. K. C. Misra for his useful suggestions throughout the project and for his critical review of the text. Special thanks go to Dr. R. H. Hunter who was particularly helpful in the interpretive aspect of this thesis, and generous with his time, and who provided a very thorough review of the text.

I am grateful to the following people who helped me in specific areas: Rich Hopkins introduced me to and ran the computer program that performed the geophysical modelling; Tom Sando performed Sm-Nd isotope dating on Concord gabbro samples and recalculated the Rb-Sr age from published data; Dr. J. R. Butler provided a copy of a reconnaissance map of the study area; he also supplied the results of the major and trace element geochemical analyses used in this thesis.

I am grateful to the Geological Sciences Department for providing financial assistance and an excellent academic atmosphere in which to conduct my graduate studies, complete this thesis and prepare for my career.

Finally I would like to thank my parents, Mr. and Mrs. Edward O. Olsen, who have always given me love and support and the confidence to reach this goal.

ABSTRACT

The Concord intrusive complex consists of a gabbro stock partially encircled by a syenite ring dike. A simple gravity model suggests that the gabbro pluton extends to a depth of about 6 km. and that the steep-walled syenite ring dike dips outwardly at an angle of 78° on the west side, and dips vertically on the east side. Isotopic data indicate that crystallization of the gabbro and syenite were approximately contemporaneous, and the close field association of these bodies suggests a relationship through fractional crystallization.

Three gabbroic rock types, based on the presence of different cumulus minerals, occur. Olivine-plagioclase cumulate (OPC) gabbros contain cumulus olivine and plagioclase, and postcumulus clinopyroxene, orthopyroxene and hornblende. Clinopyroxene-plagioclase cumulate (CPC) gabbros contain cumulus clinopyroxene and plagioclase; olivine-clinopyroxene-plagioclase cumulate (OCPC) gabbros contain cumulus olivine, clinopyroxene and plagioclase; both CPC and OCPC gabbros contain postcumulus orthopyroxene and hornblende. All gabbro types contain biotite, Fe-Ti oxides, sulfides, apatite and zircon. The syenite is a coarse-grained seriate porphyry with phenocrysts of perthitic feldspar and a groundmass of perthite, albite, microcline, clinopyroxene, amphibole, biotite, oxides, sulfides, apatite, zircon and monazite. Mafic mineral compositions in both the gabbro and syenite indicate limited Fe-enrichment trends during crystallization.

Cumulate textures suggest that the fractionation of the Concord complex parental magma was dominated by plagioclase, olivine and clinopyroxene. Petrogenetic modelling of major and trace elements indicates that the Concord syenite could be produced by 95% fractional crystallization of olivine, plagioclase and clinopyroxene in roughly cotectic proportions, with minor sulfide and oxide minerals, from a basaltic parental magma.

The Concord gabbro-syenite trend probably represents near-critical plane differentiation of a tholeiitic or transitional basaltic liquid to a syenitic residual liquid with composition close to that of the alkali feldspar join in the system $NaAlSiO_4$-$KAlSiO_4$-SiO_2. This fractionation took place at depth, before intrusion of the syenitic liquid into the fractured region between the gabbro and country rock. Fractionation from basaltic to trachytic liquid is not unusual, and it can be shown that any parental magma with composition near the plane of critical silica undersaturation is likely to exhibit this trend.

TABLE OF CONTENTS

CHAPTER		PAGE
I.	INTRODUCTION	1
	Statement of the Problem and Previous Work	1
	Analytical Techniques and Sources of Data	3
II.	GEOLOGY OF STUDY AREA	6
	Geologic Setting	6
	Field Relations	6
	Geophysical Expression	9
	A Model for Emplacement of the Complex	14
III.	MINERALOGY AND PETROGRAPHY	17
	Classification	17
	Mineralogy	20
	Textural Relations and Crystallization History	28
IV.	GEOCHEMISTRY	32
	Assumptions and Limitations of Chemical Modelling	32
	Fractionation of Major Elements	32
	Fractionation of Trace Elements	38
V.	DISCUSSION	45
	Inferences About the Parental Magma	45
	Petrogenesis	45
	Conclusions	50
LIST OF REFERENCES		52
APPENDIX		57
VITA		72

LIST OF TABLES

TABLE		PAGE
1.	Relative Proportions of Cumulus Minerals	31
2.	Average Compositions of Concord Gabbro and Syenite and Presumed Cumulus Phases	36
3.	Solution to the Petrologic Mixing Problem	39
A-1.	Modal Variations: Concord Gabbro and Concord Syenite	58
A-2.	Representative Electron Microprobe Analyses: Plagioclase	60
A-3.	Representative Electron Microprobe Analyses: Bulk Perthite	61
A-4.	Representative Electron Microprobe Analyses: Orthopyroxene	62
A-5.	Representative Electron Microprobe Analyses: Clinopyroxene	63
A-6.	Representative Electron Microprobe Analyses: Olivine	64
A-7.	Representative Electron Microprobe Analyses: Amphibole	65
A-8.	Representative Electron Microprobe Analyses: Biotite	66
A-9.	Representative Electron Microprobe Analyses: Oxides	67
A-10.	Bulk Chemical Compositions: Gabbro	68
A-11.	Bulk Chemical Compositions: Syenite	69
A-12.	Trace Element Compositions	70
A-13.	Normative Mineralogy	71

LIST OF FIGURES

FIGURE		PAGE
1.	Geologic Map of the Concord Intrusive Complex, Modified from White and Mundorff (1944) and Bell (1960)	8
2.	Aeromagnetic Contours and Areas of Anomolous Aeroradioactivity (Johnson and Bates, 1960) Superimposed on the Surface Outcrop Pattern of the Concord Syenite and Gabbro	10
3.	Gravity Data (Morgan, 1963) Superimposed on the Surface Outcrop Pattern of the Concord Syenite and Gabbro	11
4.	Comparison Between Observed and Calculated Gravity Profiles Along Section A-A' in Figure 3	13
5.	Schematic Representation of the Formation of the Concord Gabbro-Syenite Complex from a Fractionating Parental Magma Body	15
6.	Photomicrographs of Samples from the Concord Complex in Cross-Polarized Transmitted Light	18
7.	Petrologic Classification for Gabbros (Streckeisen, 1973) Showing Modal Mineralogy of OPC Gabbros, CPC Gabbros and OCPC Gabbros	21
8.	Compositions of Silicates in the Concord Gabbro and Syenite Samples	23
9.	Amphibole Classification (Leake, 1978)	26
10.	Al^{IV} vs. Total A-Site Occupancy in Amphiboles	27
11.	Expanded Normative Basalt Tetrahedron Showing Calculated Values for Concord Gabbros	34
12.	Four Representative Two-Element Variation Diagrams Showing the Gabbro-Syenite Trend	35
13.	Trace Element Variations Between Average Gabbro and Syenite	40

FIGURE PAGE

14. Rb-Sr and Rb-Zr Variation Diagrams for Concord Gabbro and Syenite 43

15. The Thermal Valley and Profile Along the Thermal Valley in Petrogeny's Residua System 47

16. Total Alkalis vs. Silica for Concord Gabbro and Syenite 49

LIST OF PLATES

PLATE

I. Geologic Map of the Concord Gabbro-Syenite Complex, Cabarrus County, North Carolina . . . . . In Pocket

CHAPTER I

INTRODUCTION

Statement of the Problem and Previous Work

Unlike other mafic plutons that are exposed in a linear chain in the Southern Appalachian Piedmont, the Concord intrusive complex, Cabarrus County, North Carolina, consists of a gabbro body closely associated with a syenite ring dike. The Mt. Carmel gabbroic complex (Medlin, 1968) is the only other Piedmont intrusive containing both gabbro and syenite. Gabbros are commonly associated with diorite in this region (Butler and Ragland, 1969), although no diorite occurs in the Concord complex. Many gabbro bodies are also accompanied by metagabbro (e.g., Clark, 1980; Hermes, 1968), but the Concord complex is unmetamorphosed.

The rocks of the Concord area were first described by Watson and Laney (1906) in a report on the ornamental and building stones of Cabarrus and Mecklenburg counties. White and Mundorff (1944) compiled a preliminary geologic map of the Concord complex. In a report summarizing the economic potential of the Concord area, Bell (1960) prepared a reconnaissance map of the Concord area. Airborn magnetic and radioactivity surveys of the Concord area were conducted by Johnson and Bates (1960). Morgan (1963) conducted a detailed gravity study of the area and gave brief petrologic descriptions. Cabaup (1969) performed bulk chemical analyses on Concord gabbro samples, and Price

(1969) determined a suite of trace elements in samples of gabbro and syenite. These geophysical and geochemical studies will be reinterpreted in light of new field and petrologic data presented here.

The crystallization age of the Concord syenite was determined to be 413 ± 21 m.y. (1σ) using the Rb/Sr technique (Fullagar, 1971). The initial $^{87}Sr/^{86}Sr$ value of 0.7038 ± 0.004 (1σ) is similar to that determined for Concord gabbro samples (0.7035). Sando (personal communication, 1981), using the Sm/Nd technique, determined an age of 407 ± 36 m.y. (1σ) for the Concord gabbro. The initial $^{143}Nd/^{144}Nd$ ratio is computed to be 0.51233 ± 0.00003 (1σ). Sando recalculated the Rb-Sr age for the syenite reported by Fullagar (1971) to be 404 ± 21 m.y. Sando found the initial ratio taken from the gabbro isochron and that calculated for the syenite using the published Rb-Sr age to be indistinguishable. It is thus clear that the Concord gabbro and syenite formed from magmas that were closely associated in space and time and have similar initial isotopic ratios.

Previous studies of the Concord complex (Morgan, 1963; Butler and Ragland, 1969; Price, 1969) have suggested that the syenite is a later differentiate of the same parental magma which produced the gabbro. This paper substantiates that theory. A fractionation trend such as this one that terminates in a syenitic liquid presents an intriguing problem: the composition of syenite lies on an apparent thermal maximum in the termary system $NaAlSiO_4$-$KAlSiO_4$-SiO_2. The composition of a differentiating basaltic melt in this system would be expected to approach one of the thermal minima at either side of this thermal

maximum (Morse, 1980). Since gabbro-syenite associations are not rare, there must be other factors influencing this fractionation trend. The "syenite problem," as it relates to the Concord complex, will be addressed in this paper.

Analytical Techniques and Sources of Data

Field mapping of the Concord area was carried out using portions of the Concord, S.E. Concord, Kannapolis and Harrisburg Quadrangle U.S.G.S. 1:24000 scale topographic maps. Approximately 120 rock samples were collected from large boulders and outcrops. As a result of poor exposure contacts between gabbro, syenite, and country rocks are not visible in the field and cannot always be precisely fixed by closely-spaced sampling. Since the syenite body is more resistant to weathering, it forms a pronounced topographic high area (about 100 ft. in relief) relative to gabbro and country rocks. This topographic distinction was used to infer contacts.

Forty-eight thin sections were prepared for petrographic study. Of these, 33 gabbro samples were point-counted, using at least 1000 points per thin section, and five syenite samples were point-counted, using at least 500 points per thin section, to determine modal percentages of minerals. In order to distinguish plagioclase from alkali feldspar, the syenite thin sections were stained with a sodium cobaltinitrate solution, according to the method of Deer et al. (1966). Modal percentages are reported in Table A-1, in the Appendix. The reliability of the results of point counting lies within a relative

lower limit of 1-10% using the chart of Van der Plas and Tobi (1965). Actual analytical error may be greater due to increased variance introduced by grid distance used, relationship of adjacent grains and layering in samples (Neilson and Brockman, 1977).

Mineral compositions were determined using an automated MAC 400S electron microprobe, with appropriate natural and synthetic standards, utilizing the correction procedures of Bence and Albee (1968) and the data of Albee and Ray (1970). Analyses were performed on minerals in nine polished thin sections, using a defocussed electron beam approximately 5 to 15 μm in diameter. Operating conditions were set at 15 kv and 0.03 to 0.05 μa beam current, depending on the mineral to be analyzed. For amphibole analyses Fe^{3+} was calculated using the method of Leake (1978), and for oxide analyses Fe^{3+} was calculated based on stoichiometric considerations.

Bulk chemical analyses for major elements in 40 Concord gabbro samples were obtained from an unpublished thesis by Cabaup (1969). Butler and Ragland (personal communication, 1980) supplied individual bulk chemical analyses for major elements for seven Concord syenite samples and six Concord gabbro samples (previously published in summary form by Butler and Ragland, 1969), and chemical analyses for trace elements on the same samples were reported in an unpublished dissertation by Price (1969). These data and the calculated normative mineralogy are reported in Tables A-10-A-13, in the Appendix. All analyses reported total Fe as Fe^{2+}; for norm calculations, $Fe_2O_3/FeO + Fe_2O_3$ ratios for average gabbro (0.24) and average syenite (0.45) (Nockolds, 1964) were used to correct the Fe values in the analyses.

Geophysical modeling was performed using gravity data from an unpublished thesis by Morgan (1963). An observed profile of the gravity configuration produced by the Concord pluton was compared to theoretical profiles produced by several models. The profiles were generated by the Talwani 2-D Gravity Program No. W9206 (Talwani et al., 1959), provided by the Geological Services Division of the Tennessee Valley Authority. This program calculates the vertical gravity component for two-dimensional bodies.

CHAPTER II

GEOLOGY OF STUDY AREA

Geologic Setting

The Concord intrusive complex occurs within the Charlotte regional belt of the southeastern Piedmont. Characterized by the occurrence of numerous igneous plutons, the crystalline rocks of the Charlotte belt are dominated by granitic and metagranitic bodies. The rocks of the Charlotte belt generally show evidence of regional metamorphism of greenschist to amphibolite facies grade (Butler and Ragland, 1969), but many intrusives, including the Concord complex, are postmetamorphic.

The study area is located in Cabarrus County, North Carolina, about 23 km northwest of Charlotte. According to Bell's (1960) interpretation, the Concord pluton is surrounded mostly by "massive and foliated dioritic and mafic rocks," with "gneissic and granodioritic rocks" in contact with the syenite body on the east and west margins of the intrusion. Field observations indicate a paucity of country rock outcrops, but saprolite observations show Bell's interpretation to be generally correct.

Field Relations

The Concord complex consists of a discontinuous syenite ring dike, with thickness varying between 0.5 and 2.5 km, partially encircling a gabbro body of roughly oval shape, with dimensions of about 10.8 km

from north to south and 6.7 km from east to west. Both rock types are cut by numerous pegmatite dikes of random orientation. Within the complex, a few Mesozoic diabase dikes cross-cut the gabbro. Figure 1 is a geologic map of the study area, based on this work and modified from Bell (1960) and an unpublished map by White and Mundorff (1944). The latter map, which shows the syenite body to be continuous at the surface across the northern end of the pluton, is in disagreement with the Concord Quadrangle map of Bell (1960). Bell's map denotes a parentheses shape for the syenite body, open at the northern and southern ends. Field studies reveal syenite outcrops and quarries at this northern end, which confirm the horseshoe-shaped ring dike described earlier by White and Mundorff (1944).

The Concord gabbro is exposed mainly as large, spheroidally weathered, bluish-black boulders in stream channels, float piles and pastures. The Concord syenite is found in regions of topographic elevation. It is exposed mainly as pedestal-shaped boulders, although a few outcrops occur, and quarries provide abundant fresh samples. The tannish-gray syenite boulders are much larger than the gabbro boulders and are more extensively weathered. Large feldspar phenocrysts stand out in relief on the surfaces of weathered samples. Due to the paucity of outcrops, contacts between the gabbro and syenite, the syenite and country rock, and the gabbro and country rock have not been found. There is, however, geophysical evidence which is useful in determining the location of contacts at the surface, as well as suggesting a shape for the pluton at depth.

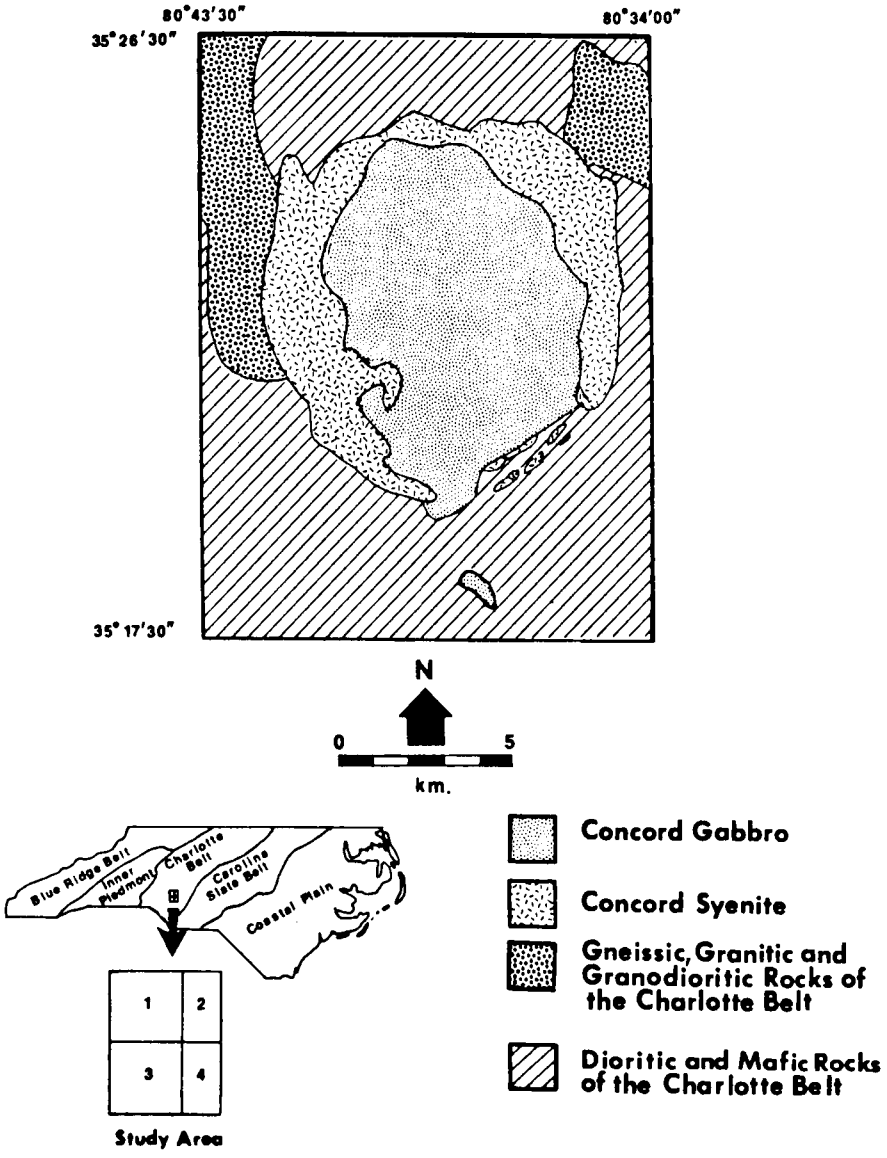

Figure 1. Geologic map of the Concord intrusive complex, modified from White and Mundorff (1944) and Bell (1960). The inset map of North Carolina shows the location of the study area in the Charlotte Regional Geologic Belt. The study area is comprised of portions of the four quadrangles shown: Kannapolis quadrangle (1), Concord quadrangle (2), Harrisburg quadrangle (3), and Concord S.E. quadrangle (4).

Geophysical Expression

The results of two geophysical studies conducted in the Concord area are available for comparison and reinterpretation. The first is an aeromagnetic and aeroradioactivity survey of the Concord quadrangle by Johnson and Bates (1960). This study produced two maps with contoured anomalies which have been compared with the outcrop pattern of the complex in Figure 2. On the magnetic map (Figure 2a), a group of closely-spaced contours coincides with the boundaries of the syenite body. Johnson and Bates suggested that magnetite concentrated along the contacts between the gabbro and syenite produces the extensive 4500 gamma anomaly that surrounds the gabbro body. Smaller gabbro bodies extending out from the southern end of the pluton, which are shown on Bell's (1960) map, also coincide with magnetic anomaly patterns. The radioactivity map (Figure 2b) shows the syenite body outlined by two parentheses-shaped areas of high radioactivity.

The second geophysical report is a detailed gravity study of the Concord area by Morgan (1963). Morgan's thesis included calculations of the Bouguer anomalies for the area, from which he produced three maps showing the simple Bouger anomaly (Figure 3a), the residual anomaly (Figure 3b) and the gradient anomaly (not illustrated). Correlation between the geologic structures and the gravitational configuration of the simple Bouguer anomaly map (Figure 3a) is obvious. The gabbro intrusion shows a pronounced increase in Bouguer value, reaching a maximum of 36.5 milligals in the center. The simple Bouguer anomaly map reflects large scale regional trends and deep-seated mass

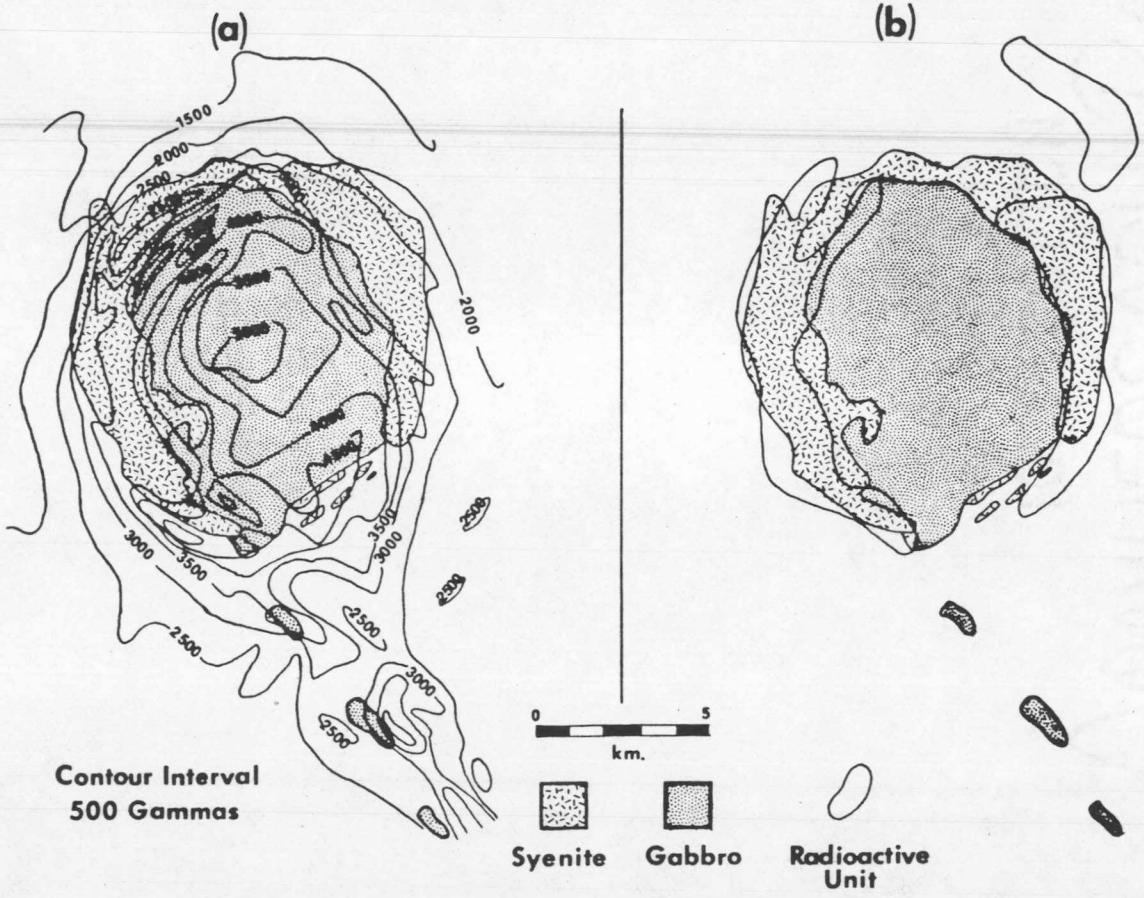

Figure 2. (a) Aeromagnetic contours and (b) areas of anomolous aeroradioactivity (Johnson and Bates, 1960) superimposed on the surface outcrop pattern of the Concord syenite and gabbro.

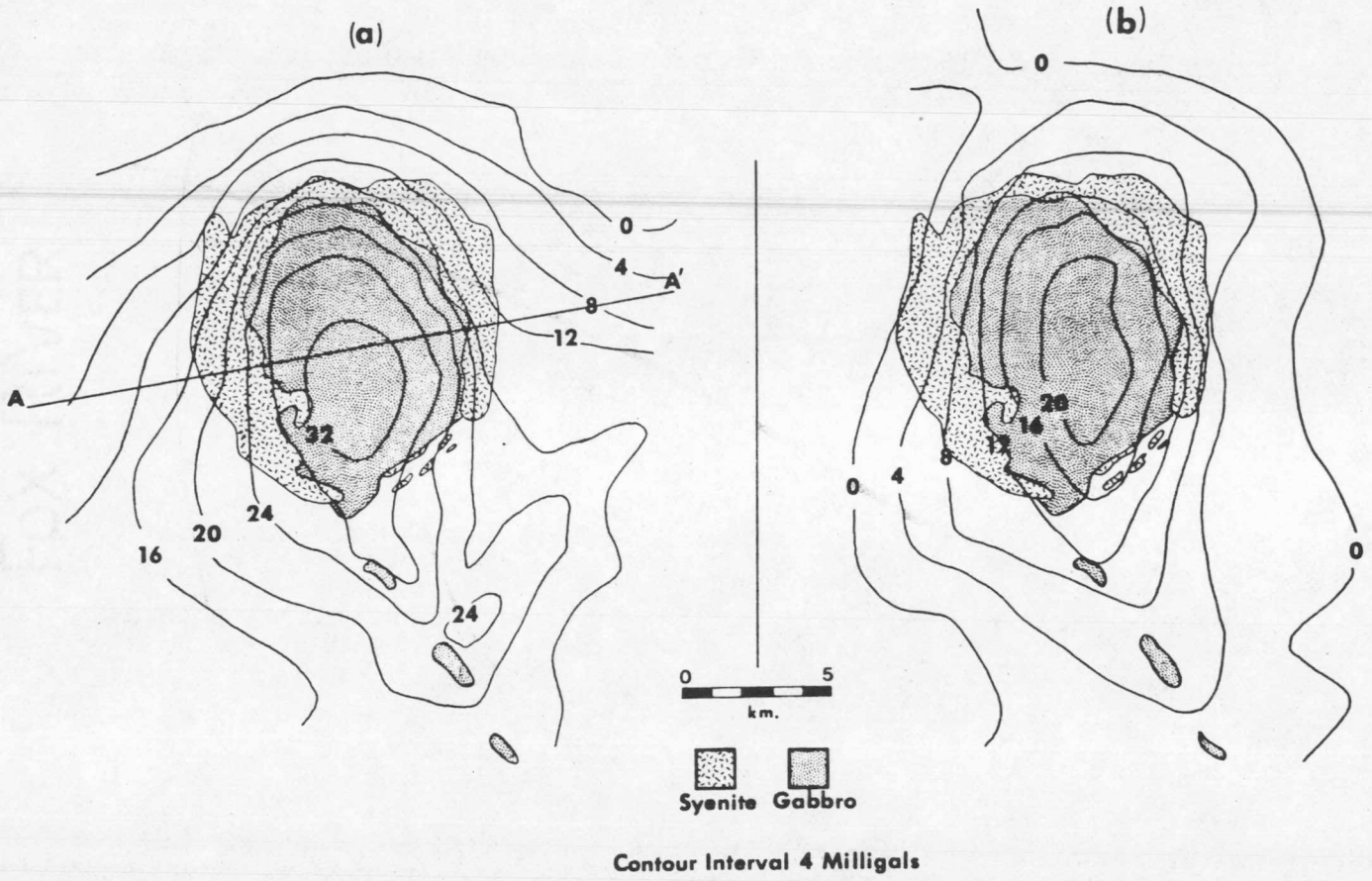

Figure 3. Gravity data (Morgan, 1963) superimposed on the surface ourcrop pattern of the Concord syenite and gabbro. (a) Simple Bouguer anomaly map. (b) Residual anomaly map. Line A-A' in (a) was used to produce the gravity profile.

distributions. This map can be used to estimate the shape of the body at depth. The residual anomaly map (Figure 3b) represents the gravitational distribution of local shallow geologic structures. The contours shown on this map roughly outline the shape of the body at the surface. The gradient anomaly map, a refinement of the residual anomaly map, also represents near-surface mass distributions, and should correlate closely with the surface expression of the pluton. In this map, an 8 milligal contour outlines the horseshoe shape of the syenite body. The trend of isolated gabbro bodies extending from the open southern end of the intrusion is reflected in all three gravity maps, suggesting these smaller intrusions are related to the main gabbro body at depth.

The detailed nature of this gravity study provided the opportunity to construct a gravity profile and propose a simple model for the geometry of the pluton at depth. An observed gravity profile was constructed along line A-A', shown on the simple Bouguer anomaly map in Figure 3a. This particular line was chosen because it produced the most symmetrical profile (Figure 4). Several simple geologic models were constructed using estimated specific gravity values for the different rock types, and by varying (a) the dip angle and direction of the syenite dike, and (b) the depth to the bottom of the pluton. Theoretical gravity profiles were generated through a program using the technique of Talwani et al. (1959). Figure 4 shows the profile that most closely resembles the observed gravity profile, and the model which produced this profile. This configuration depicts a steep-walled syenite ring dike with an outward dip of 78° on the west

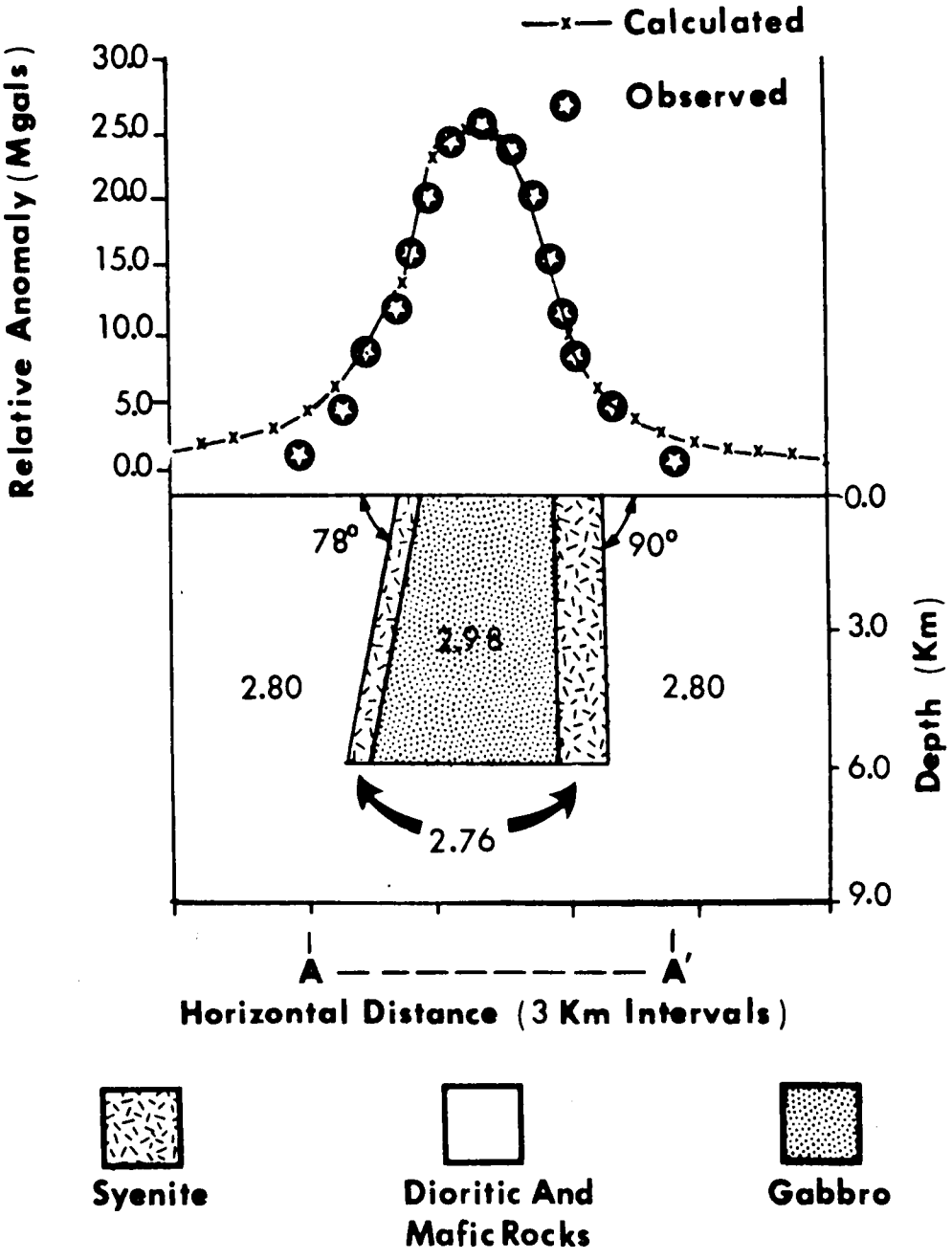

Figure 4. Comparison between observed and calculated gravity profiles along section A-A' in Figure 3. Calculated profile assumes the geometry and rock densities indicated.

side and vertical dip on the east side, and a depth of about six kilometers to the bottom of the pluton. An even more refined fit would be obtained if the syenite were modeled as a wedge thickening downward rather than a plate of uniform thickness.

Hermes (1968), Chalcraft (1970), and Wilson (1981) performed geophysical modelling of gabbroic plutons in the Charlotte Belt. In the Mecklenburg gabbroic complex (Hermes, 1968), the gabbro occurs as a nearly circular stock, with a surface area of about 33 km^2. Hermes assumed a cylindrical plug shape for the gabbro body, and using gravity data determined a depth of between 2.4 and 5 km, depending on gabbro density. In a more recent study, Wilson (1981) calculated a thickness of 3.5-4.5 km for the Mecklenburg pluton. The Rock Hill gabbro pluton (Chalcraft, 1970) outcrops over about 40 km^2. Assuming a vertical cylinder shape for the pluton, Chalcraft used magnetic data to determine a depth of about 3.4 km. Considering the relative sizes of the three plutons, the depths given by the three separate studies appear to be roughly comparable, although the Concord complex may extend to slightly deeper levels.

A Model for Emplacement of the Complex

A reasonable sequence of events that would produce the structure suggested by the geophysical model for the Concord complex begins with the intrusion of mafic magma to form a gabbro stock. This pulse of magma would be derived from a large body of magma at depth prior to significant fractionation (Figure 5a). A syenitic residual liquid

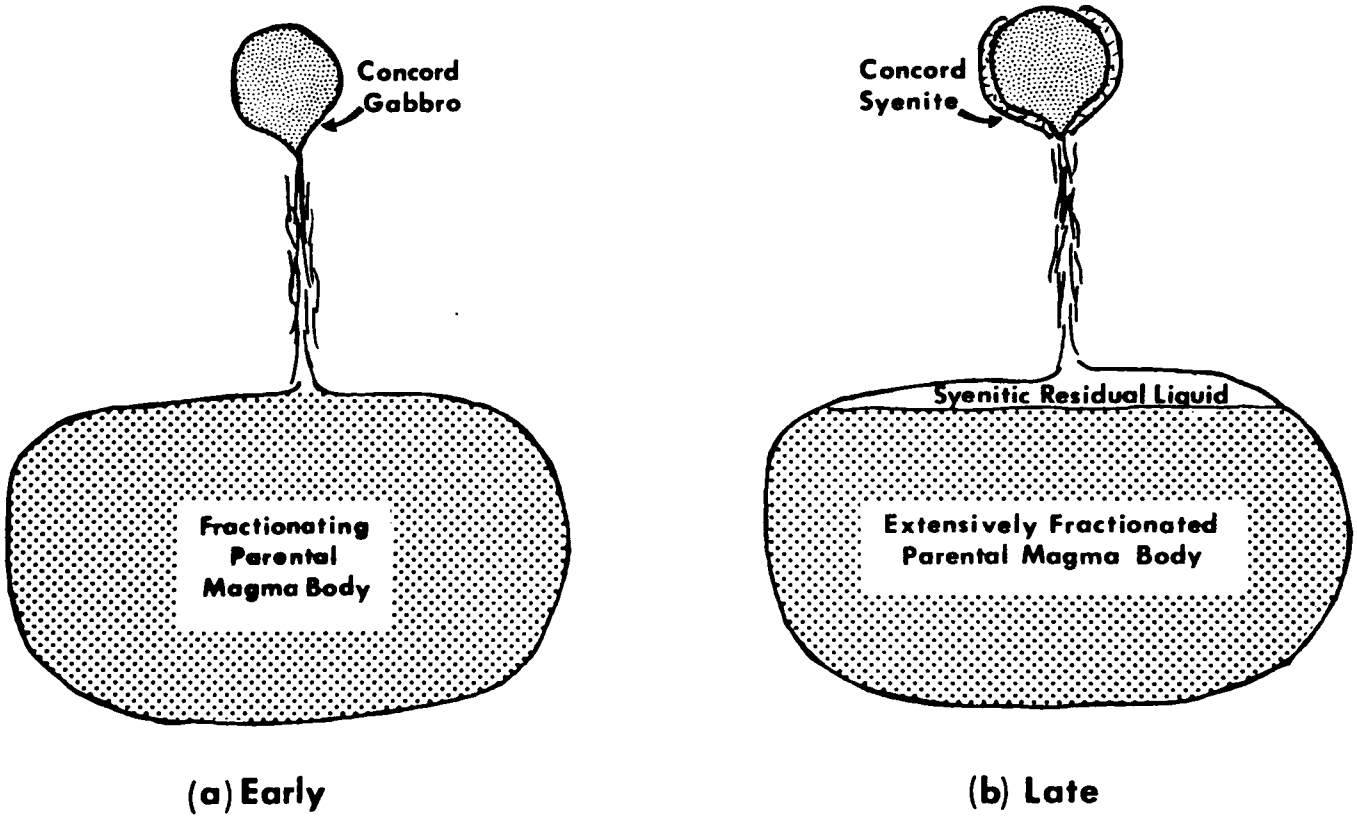

Figure 5. Schematic representation of the formation of the Concord gabbro-syenite complex from a fractionating parental magma body.

might be produced by extensive fractionation of the source magma body at depth as suggested by Morgan (1963), Butler and Ragland (1963) and Price (1969). A fractured region around the contact between the gabbro and country rock was subsequently intruded by this syenitic magma (Figure 5b). That the ring dike does not form a complete ring may be explained by the presence of smaller gabbro bodies extending out from the open southern end of the pluton. The geophysical maps suggest that these bodies may be continuous at depth with the main gabbro body. They may represent outcrops of a sill-like projection of gabbro at this southern end, which might have prevented the syenite from intruding as a complete ring dike. The presence of two discrete alkali feldspars in the syenite indicate the complex was emplaced at depths of approximately 15 km or greater. Testing of the inferred petrologic relationship between the Concord gabbro and syenite will be the focus of the remainder of this paper.

CHAPTER III

MINERALOGY AND PETROGRAPHY

Classification

Concord gabbro samples contain plagioclase, olivine, clinopyroxene, orthopyroxene, and amphibole, with lesser amounts of biotite, oxide minerals, sulfides, apatite, and zircon. Sericite, serpentine and chlorite occur as minor alteration products. Three major gabbroic rock types are recognized, distinguished by the presence of different cumulus minerals. The first type contains cumulus olivine and plagioclase poikilitically enclosed by postcumulus orthopyroxene, clinopyroxene, and hornblende (Figure 6a). This type will be referred to as olivine-plagioclase cumulate (OPC) gabbro. As the proportion of intercumulus material decreases, these rocks grade into troctolitic gabbros. The second gabbroic rock type is clinopyroxene-plagioclase cumulate (CPC) in which these phases are poikilitically enclosed by postcumulus orthopyroxene and hornblende (Figure 6b). In this rock type clinopyroxene does not occur as oikocrysts. Samples which contain all three cumulus phases are olivine-clinopyroxene-plagioclase cumulates (OCPC). Areal distributions of OPC, CPC and OCPC samples and of syenite are shown in the geologic map (in pocket).

Modal proportions of the major phases (see Table A-1, in the Appendix) can be compared using the classification system recommended by the I.U.G.S. (Streckeisen, 1973). The gabbroic rocks are norites

Figure 6. Photomicrographs of samples from the Concord complex in cross-polarized transmitted light.

(a) Cumulus olivine and plagioclase in OPC gabbro.
(b) Cumulus clinopyroxene and plagioclase and postcumulus amphibole in CPC gabbro.
(c) Zoned perthite phenocryst with augite and Fe-Ti oxide inclusions in syenite.
(d) Porphyritic texture in syenite, with perthite phenocrysts and groundmass of plagioclase, microcline, quartz, and interstitial augite, amphibole and oxides.

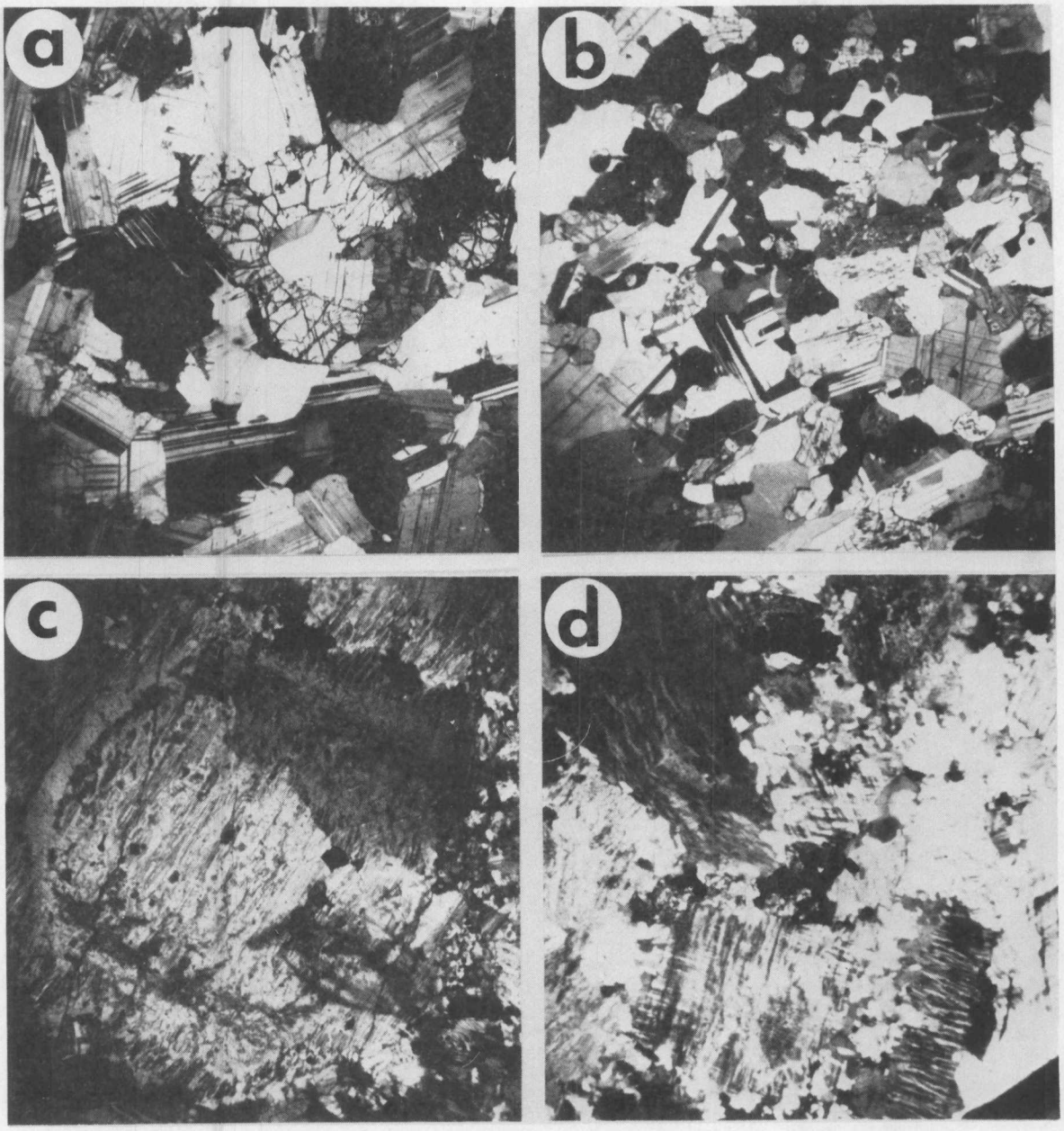

Figure 6.

and gabbronorites, according to modal clinopyroxene/orthopyroxene ratios (Figure 7). OPC samples generally fall within the norite field of Figure 7, and CPC and OCPC samples are generally within the gabbronorite field. This diagram is a graphical representation of modal variations. In this paper the term "gabbro" with appropriate modifiers to indicate cumulus phases will be used for classification.

The Concord syenite is a coarse-grained, seriate porphyry containing large phenocrysts of perthite and antiperthite (Figure 6c) in a groundmass of perthite, plagioclase, microcline, clinopyroxene, biotite, amphibole, quartz, oxide and sulfide minerals, zircon, apatite and monazite (Figure 6d). The mafic minerals and opaques tend to occur as intergranular clusters. Modal proportions of the major minerals fall within the syenite field of the I.U.G.S. classification system (Streckeisen, 1973).

Mineralogy

Plagioclase is the dominant mineral modally in the gabbro samples, but is of lesser abundance in syenites. Individual grains are normally zoned and partially altered to sericite in the cores, and frequently contain inclusions of euhedral apatite. Gabbroic plagioclases range in composition from An 77-31, and syenitic plagioclases range from An 15-1. This compositional range is more restricted within any specific sample, as shown in Figure 7.

Alkali feldspar is absent in gabbro samples, but is present in syenite as microcline and both perthite and antiperthite are present.

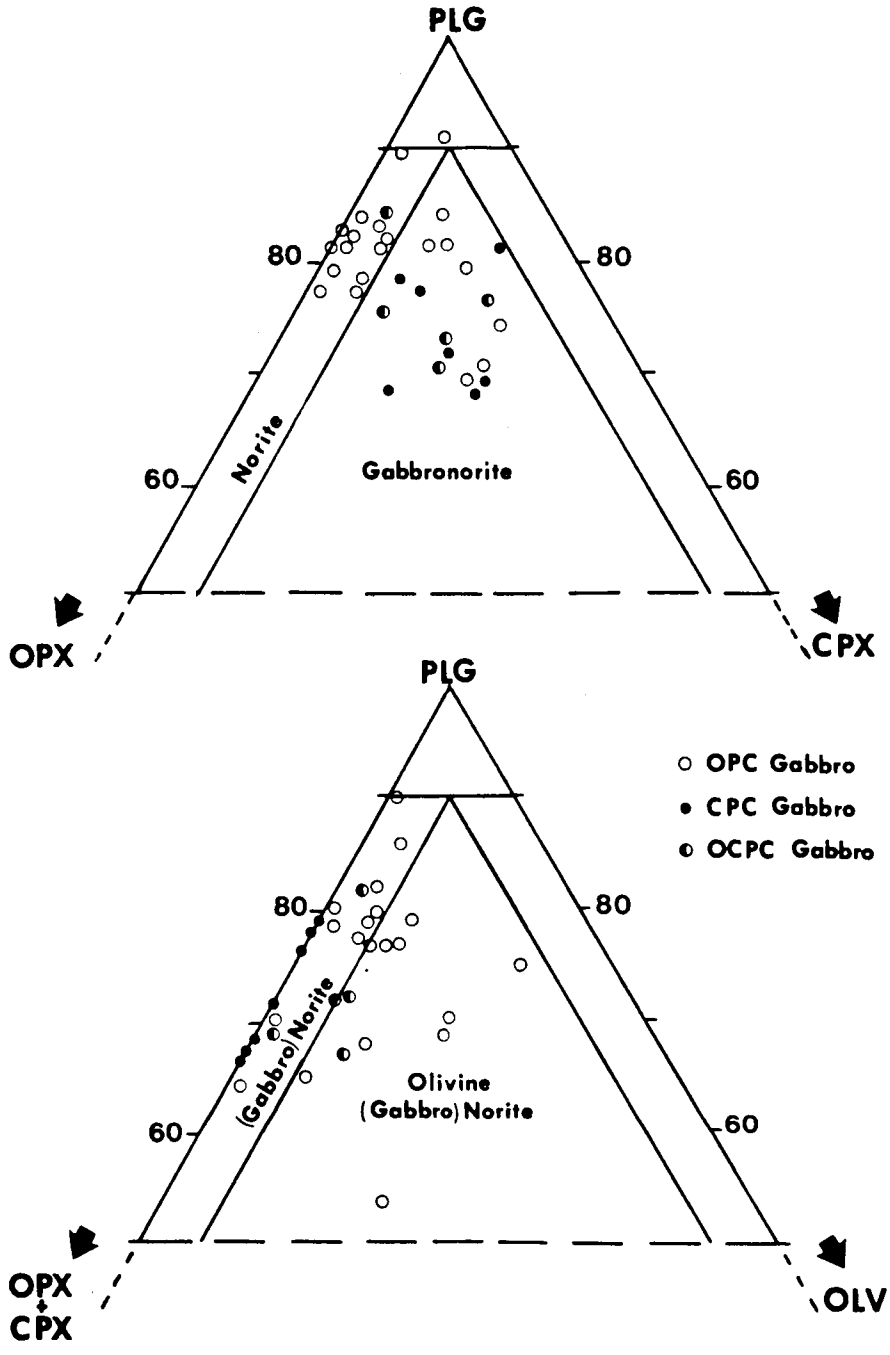

Figure 7. Petrologic classification for gabbros (Streckeisen, 1973) showing modal mineralogy of OPC gabbros (open circles), CPC gabbros (filled circles) and OCPC gabbros (half-filled circles).

Perthite and antiperthite were distinguished in stained samples, but in unstained samples the lamellae are so fine that it is difficult to determine which component is the host mineral and which is the exsolved phase. Some perthitic feldspars are strongly zoned, with perthitic cores surrounded by bands of sodic plagioclase, followed by perthitic rims. Perthitic grains contain similar amounts of alkali feldspar (Or 97-15) and sodic plagioclase (An 16-1). Some perthitic grains contain dusty zones of sericite and clay inclusions that form an internal outline of the external crystal shape. Clinopyroxene, apatite and oxide minerals are present as inclusions in perthite.

Orthopyroxene is the dominant pyroxene in many gabbro samples, but it does not occur in the syenites. It is slightly pleochroic from green to pink and occurs as large oikocrysts enclosing plagioclase, olivine, and less commonly clinopyroxene. The orthopyroxenes are bronzites (Figure 8), and many grains contain lamellae of clinopyroxene exsolved along (100) cleavage. Orthopyroxene forms thin reaction rims around olivine, and is intergrown with magnetite and ilmenite to form symplectite. This intergrowth normally occurs at the edge of an olivine grain that is surrounded by hornblende, an indication that the orthopyroxene-magnetite/ilmente symplectite is a result of a reaction between olivine and residual melt (Ambler and Ashley, 1980; McSween, 1980; Garrison and Taylor, 1981). Plate-like lamellae of ilmenite also occur in the orthopyroxene, oriented along the (010) plane. Similar textures have been observed in other gabbro bodies (McSween, 1980; Garrison and Taylor, 1981).

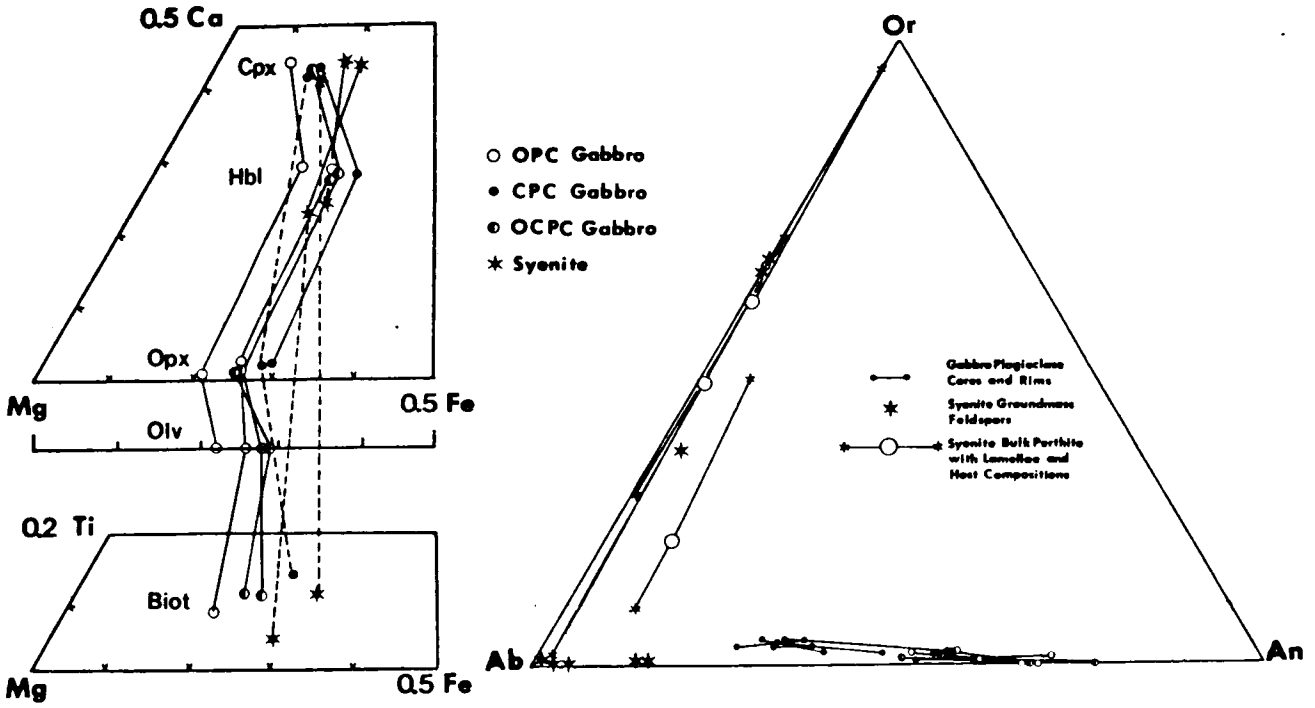

Figure 8. Compositions (mole %) of silicates in the Concord gabbro and syenite samples. Ferromagnesian minerals coexisting in the same samples are joined by tie-lines. In the feldspar diagram, individual plagioclase cores and rims in gabbro samples are joined by tie lines. Bulk perthite compositions in syenite are joined to corresponding lamellae and host compositions by tie lines.

Clinopyroxene occurs in gabbros either as oikocrysts surrounding plagioclase and olivine, or less frequently as discrete subhedral to anhedral grains. Clinopyroxene is present in the groundmass of syenite samples in clots of mafic minerals. In both rock types its composition is augite, although the syenite augites are more Fe-rich (Figure 8). This mineral contains exsolution lamellae of orthopyroxene, parallel to (100). In the gabbroic clinopyroxenes, magnetite and ilmenite lamellae form thin platelets parallel to the (010) plane.

In the gabbro, subhedral to anhedral olivine grains are intergrown with plagioclase laths and frequently rimmed by pyroxene and hornblende. Most olivine is replaced along fractures by magnetite, iddingsite and serpentine, and some grains have been partially to totally replaced by orthopyroxene, chlorite or serpentine. Olivine within the pluton ranges in composition from Fo 78-70 (Figure 8), but has uniform composition within any one specimen. No compositional zoning occurs in individual grains. Although fayalitic olivine is common in some syenites (e.g. Parsons, 1979), no olivine occurs in the Concord syenite.

Large oikocrysts of amphibole, pleochroic from reddish-brown to tan, are associated with pyroxene and oxide minerals, and may form as a replacement of pyroxene. In syenite samples, amphibole occurs as discrete anhedral to subhedral grains in the groundmass (green in color), or as rims around clinopyroxene (reddish-brown in color). Compositions in terms of Ca, Mg and Fe are shown in Figure 8. According to the amphibole classification system of Leake (1978), the gabbro amphiboles can be classified as pargasites and hastingsites, and the

syenitic amphiboles can be classified as magnesio- or actinolitic hornblendes (Figure 9). A plot of Al^{IV} versus A site occupancy (Figure 10) suggests that the syenitic amphibole compositions exhibit the same pargasite-hornblende substitutions as the gabbroic amphiboles, though to a lesser degree. This may result because the syenitic amphiboles must compete with alkali feldspars for alkali elements.

In the gabbroic rocks, biotite occurs as tabular grains and sheaths, and rarely as oikocrysts in samples containing little hornblende. Biotite commonly surrounds oxide minerals in the gabbro. Biotite is present in syenite in small amounts as discrete ragged flakes or as massive sheaths clustered with other mafic minerals. Biotite in the syenite is pleochroic in shades of reddish-brown to brown or pale green to green; only the reddish-brown variety occurs in gabbro. Figure 8 shows a sympathetic variation of Ti with Fe in the biotite samples analyzed.

Quartz is absent in these gabbros, and is present in small amounts in the syenite, mostly as myrmekitic intergrowths with albite.

Magnetite and ilmenite occur in the gabbros as interstitial subhedral grains or as euhedral to subhedral inclusions in cumulus and postcumulus minerals. In syenites, these oxides occur in clusters with other mafic minerals. Composite magnetite and ilmenite grains are commonly joined by a boundary, along which a thin rim of pleonaste is normally found. Magnetite grains may contain thin straight lamellae of exsolved ilmenite.

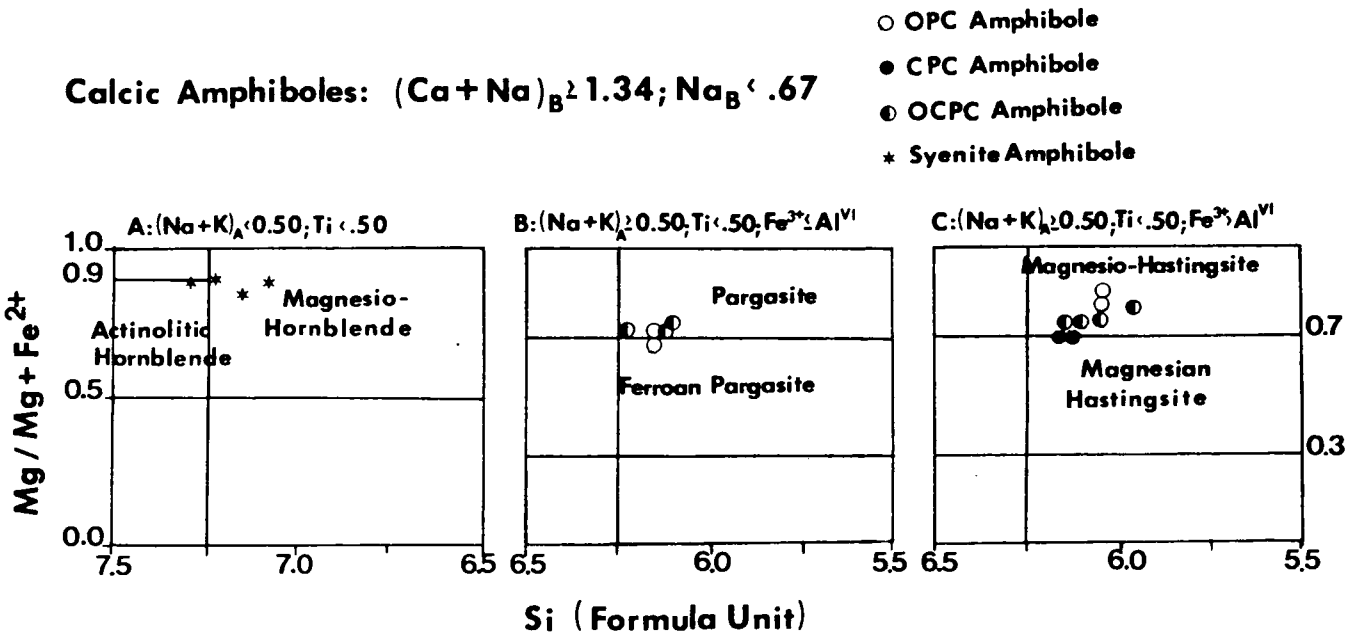

Figure 9. Amphibole classification (Leake, 1978). Gabbroic amphiboles are pargasites and hastingsites; syenitic amphiboles are magnesio- or actinolitic hornblendes.

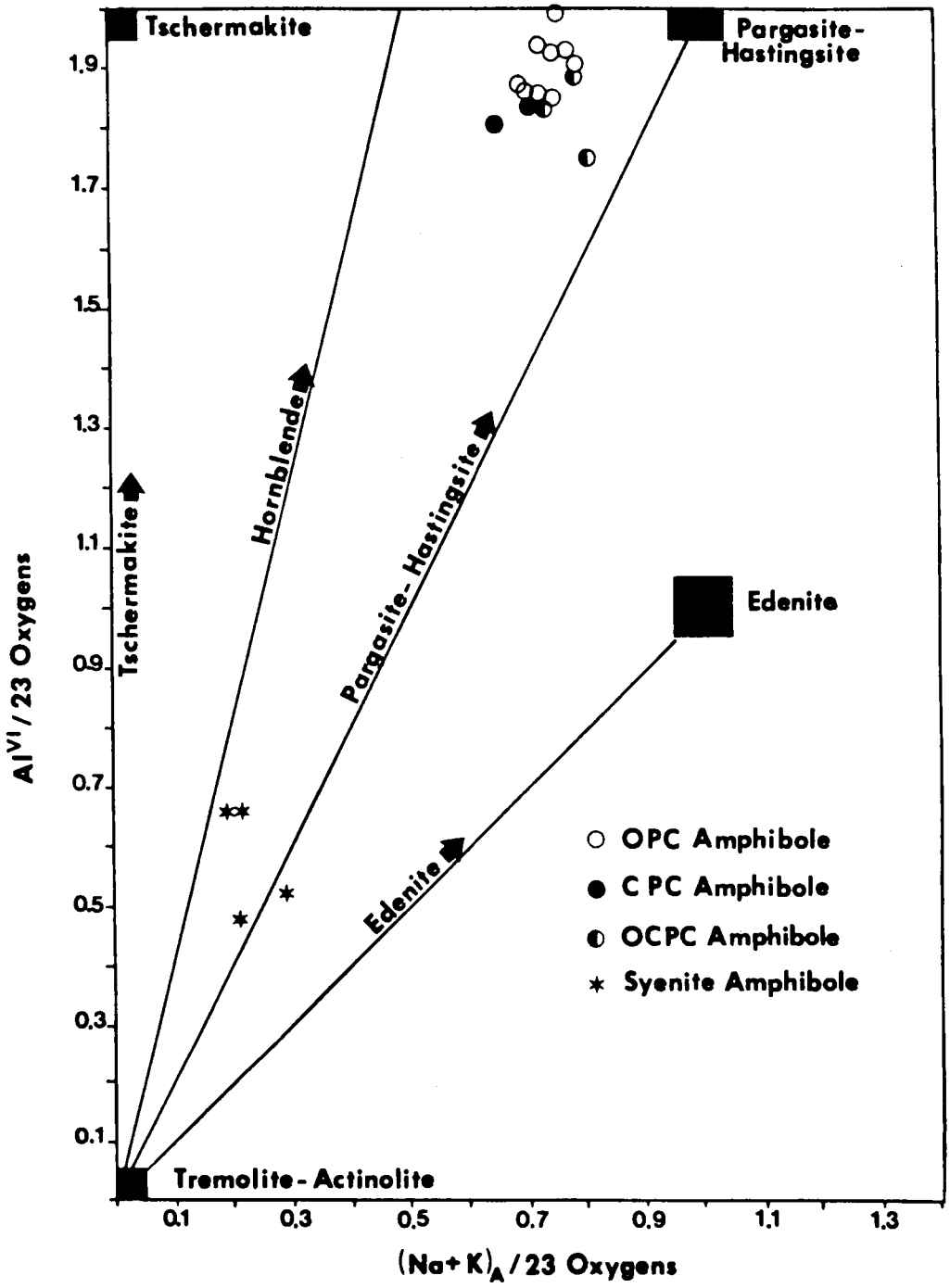

Figure 10. Al^{IV} vs. total A-site occupancy in amphiboles. Gabbroic and syenitic amphiboles exhibit pargasite-hornblende substitutions.

Sulfide minerals occur as rounded blebs in all samples. Pyrrhotite, the dominant sulfide phase, is closely associated with lesser amounts of pyrite, chalcopyrite and pentlandite in the gabbro. In the syenite, pyrite is the only sulfide mineral.

Other accessory minerals in gabbro and syenite include apatite, which forms euhedral laths and prisms, mostly interstitial, but also as inclusions in feldspars. Minute zircon inclusions in biotite produce pleochroic haloes. Plagioclase grains contain veinlets and patches of sericite as an alteration product, and chlorite and serpentine are present as alteration products of pyroxene and olivine.

Textural Relations and Crystallization History

Concord gabbro samples are predominantly mesocumulates, with lesser amounts of orthocumulates. Identification of phases as cumulus connotes only texture, as utilized by Wager et al. (1960), and does not necessarily imply settled crystals.

In OPC gabbro, olivine and plagioclase are the cumulus phases, poikilitically enclosed by postcumulus orthopyroxene, clinopyroxene and hornblende. In CPC gabbro, clinopyroxene and plagioclase are cumulus minerals, surrounded by oikocysts of orthopyroxene and hornblende. In OCPC gabbro, olivine, clinopyroxene and plagioclase are the cumulus phases, and orthopyroxene and hornblende are postcumulus. In OPC and OCPC gabbro, olivine grains are partially replaced by orthopyroxene, implying a reaction relationship between olivine and the melt. Amphibole forms large oikocrysts and replaces pyroxene.

This textural evidence indicates that olivine and plagioclase were the first minerals to crystallize, forming cumulus crystals. Inclusions of Fe-Ti oxides and apatite within cumulus phases imply they may have also crystallized early. Postcumulus material crystallized to form oikocrysts of clinopyroxene and orthopyroxene. Hornblende formed by late magmatic replacement of postcumulus pyroxene. Biotite also crystallized from the magma late in the sequence, or by reaction of oxides with residual melt. As the magma evolved during fractionation, olivine went into reaction relationship with the melt, and clinopyroxene and plagioclase were the co-precipitating phases. Orthopyroxene oikocrysts formed from intercumulus liquid. Late magmatic replacement of pyroxenes produced hornblende.

This textural sequence would imply formation of cumulate rocks in the following order: OPC gabbro; OCPC gabbro; CPC gabbro. This sequence is corroborated by Fe-enrichment in the ferromagnesian minerals, and by Na-enrichment in plagioclase cores (Figure 8, p. 23).

The syenite has a porphyritic texture containing feldspar phenocrysts and clusters of clinopyroxene, amphibole and biotite in the groundmass. The early-formed clinopyroxene grains are subhedral, fractured, and often rimmed by amphibole. The absence of orthopyroxene in syenite indicates that orthopyroxene ceased to crystallize from the liquid at some intermediate stage.

The evidence given by gabbroic textures suggests that the fractionation of the Concord early magma was controlled by plagioclase, olivine and clinopyroxene crystallization. Because most samples contain

only two of the three cumulus phases, it is difficult to estimate the proportions of those three minerals in the fractionating assemblage. The average mode of all analyzed gabbro samples is presented in Table 1. Olivine and clinopyroxene are in approximately a cotectic ratio (Table 1), but plagioclase is too abundant. However, it is almost certain that a portion of the plagioclase is postcumulus, either as zoned overgrowths on cumulus crystals or as crystals nucleated from postcumulus liquid. The proportions of the fractionating phases may be better estimated from geochemical arguments in the next section.

Table 1. Relative Proportions of Cumulus Minerals

	OPC Modes (20)[a]	CPC Modes (7)	OCPC Modes (6)	Avg. Modes[b]	Extract Diagrams[c]	Magma Mixing[d]	Cotectic Proportions[e]
Plag	86	81	84	84	57-61	57	55-60
Olv	7	-	11	5	13-25	19	10-15
Cpx	6*	18	5	10	15-30	18	25-30
Mt	0.5	0.9	0.1	0.7	-	4	-
Ilm	0.5	0.3	0.1	0.3	-	2	-

[a]Units in ( ) represent number of samples point-counted. Values are recalculated at 100%.

[b]Average modes are weighted averages of all gabbro point counts.

[c]Ranges of mineral porportions from Figure 12e, p. 35.

[d]Mineral proportions given by computed solution of the petrologic mixing calculations.

[e]Cotectic proportions of plag, olv, and cpx from McCallum et al. (1980).

*All Cpx in OPC gabbro is postcumulus.

CHAPTER IV

GEOCHEMISTRY

Assumptions and Limitations of Chemical Modelling

The following necessary assumptions may limit the conclusions drawn from this section:

1. It is clear that the Concord syenite was not derived directly by fractionation from the Concord gabbro in situ. But both may have been derived from a common parental magma. It is assumed that the gabbroic magma was extracted from such a common parental magma chamber before significant fractionation occurred.

2. It is assumed that the averages of all analyzed samples of gabbro and of syenite represent the bulk compositions of these two magmas. Because the gabbro samples are mesocumulates and orthocumulates this assumption may only be partly correct for major elements, and may be even less valid for trace elements.

3. It is assumed that the identity and compositions of the cumulus minerals in the Concord gabbro are the same as those in the larger fractionating parental magma chamber. This should be true if the chamber were tapped early to form the gabbro.

Fractionation of Major Elements

Whole rock chemical analyses (Cabaup, 1969; Butler and Ragland, 1969) and calculated normative mineralogy for 46 gabbro samples and

7 syenite samples are tabulated in Tables A-10, A-11, and A-13, in the Appendix. Most gabbro samples are hypersthene-normative, although some are nepheline-normative. Most syenites are nepheline-normative, and half the samples are acmite-normative, yet syenite samples contain modal quartz and no nepheline. The modal quartz, however, is generally in the form of myrmekitic intergrowths with albite, which is probably a secondary mineralogic feature. The presence of small amounts of modal silica-undersaturated biotite and hornblende may result in silica-undersaturation in normative calculations. Normative values for Concord gabbros are shown on an expanded normative basalt tetrahedron in Figure 11.

In any chemical fractionation diagram relating Concord gabbro and syenite, there will be a gap between clusters of points, because there are no samples with intermediate compositions. For this reason the exact differentiation path between gabbro and syenite cannot be determined. However, the identification and relative proportions of crystallizing phases which may have dominated the fractionation sequence can be estimated from major element chemistry and mineralogy of the two end members. Four representative two-element variation diagrams are illustrated in Figure 12 a-d, using average gabbro and syenite compositions (Table 2). These variations have been interpreted using the extraction method of Cox et al. (1979). Average mineral compositions for olivine and clinopyroxene and the average plagioclase composition from the samples with the most calcic plagioclase (Table 2) were used to construct the extract polygons (small triangles in Fig. 12 a-d).

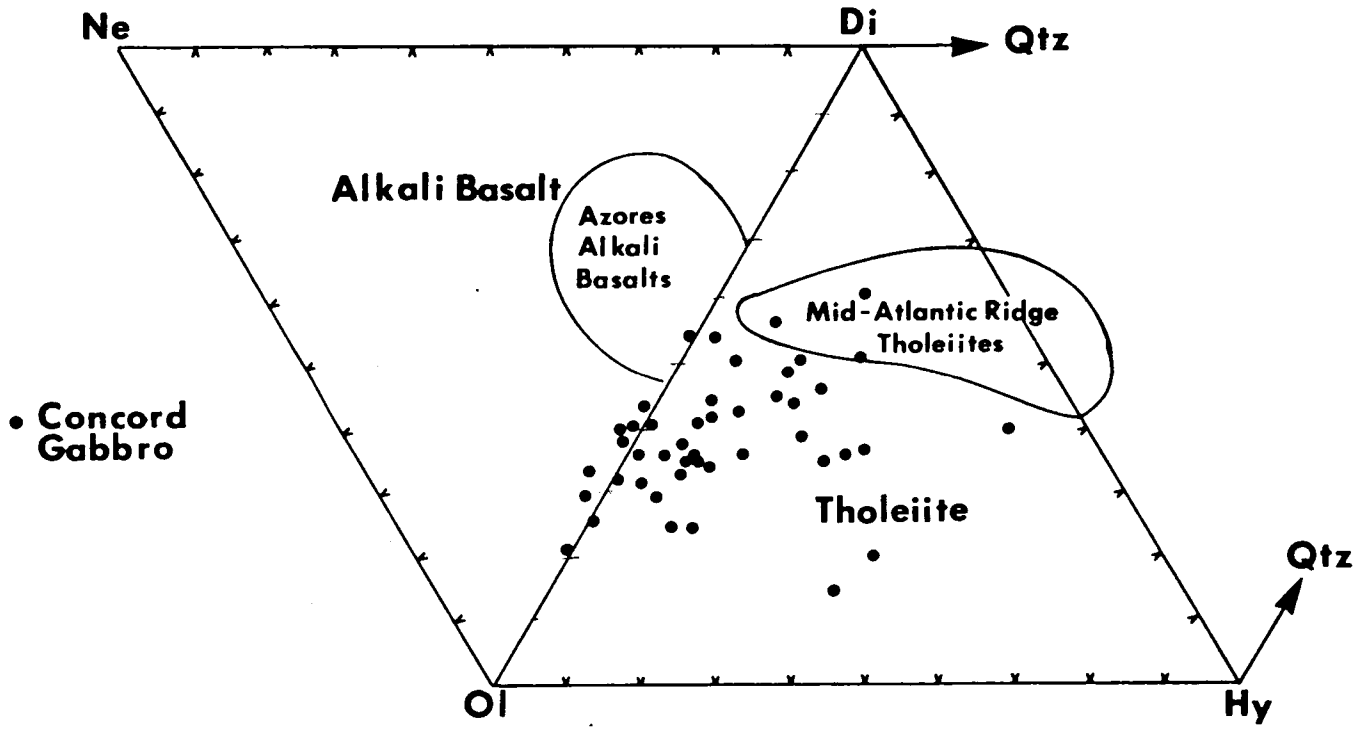

Figure 11. Expanded normative basalt tetrahedron showing calculated values for Concord gabbros. Compositions generally cluster about the Di-Ol join, the boundary between the tholeiitic and alkali basalt fields.

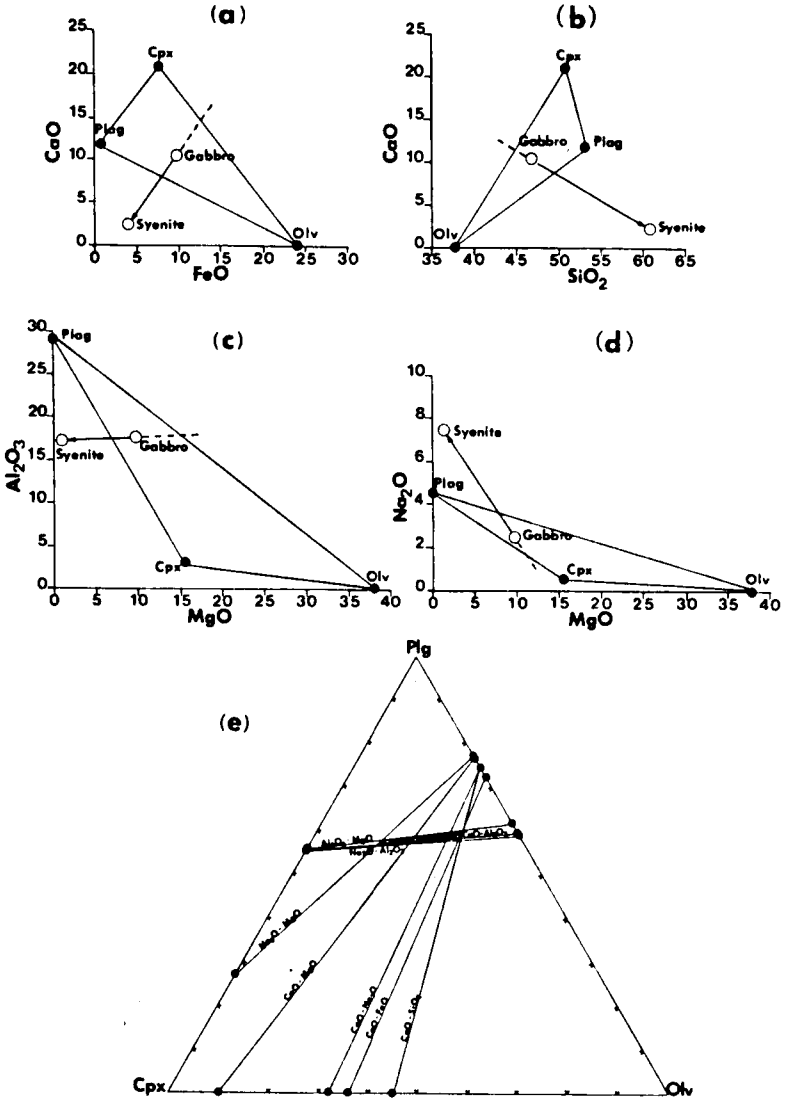

Figure 12. Four representative two-element variation diagrams (a-d) showing the gabbro-syenite trend. In each diagram this trend can be produced by extracting a mixture of plagioclase, clinopyroxene, and olivine of the same compositions as observed in cumulate gabbro phases. (e) Relative proportions of plagioclase, clinopyroxene and olivine required to produce the gabbro-syenite trend in eight extraction diagrams. Shaded area, the region of overlap, represents the range of mineral proportions in the assemblage most likely to produce this fractionation pattern.

Table 2. Average Compositions (Weight % Oxides) of Concord Gabbro and Syenite and Presumed Cumulus Phases

	MnO	FeO[d]	K_2O	CaO	TiO_2	Na_2O	MgO	Al_2O_3	SiO_2	Total
Syenite	0.19(0.02)	3.95(1.05)	4.41(1.23)	2.26(1.21)	1.05(0.29)	7.45(0.49)	1.27(0.64)	17.10(0.40)	60.8 (2.20)	98.48
Gabbro	0.14(0.03)	9.73(1.88)	0.31(0.19)	10.47(1.02)	1.20(0.38)	2.51(0.29)	9.59(2.00)	17.59(1.80)	46.9 (1.50)	98.44
Olivine	0.49	23.95	-	-	-	-	38.07	-	37.54	100.05
Plagioclase[e]	-	0.24	0.23	11.76	-	4.43	-	29.45	53.19	99.30
Plag (An 70)[f]	-	0.23	0.08	14.04	-	3.29	-	31.39	50.01	99.04
Plag (An 39)	-	0.21	0.57	7.63	-	6.61	-	25.20	59.07	99.29
Clinopyroxene	0.46	7.43	-	21.23	0.85	0.55	15.39	3.19	50.95	100.05
Magnetite	-	90.51	-	-	3.54	-	0.50	0.77	-	95.32
Ilmenite	-	41.66	-	-	51.92	-	2.91	0.09	-	96.58

[a] Average syenite and gabbro values from data of Cabaup (1969) and Butler and Ragland (1969).

[b] Units in ( ) represent one standard deviation.

[c] Average mineral compositions from electron microprobe analyses (Appendix Tables A-2 through A-9).

[d] Total Fe as FeO.

[e] Average of plagioclase analyses from sample with most calcic plagioclase.

[f] An 70 and An 39 are the most sodic and calcic values measured, used in the mixing program.

The average syenite composition can be produced by fractionation of plagioclase + olivine + clinopyroxene, as the extract composition in each of these diagrams falls within the polygon they define, but syenite cannot be produced by fractionation of any two of these phases. This is in agreement with textural evidence (cited above) which suggests that these three minerals are cumulus phases in the gabbro. The extraction diagrams are also consistent with fractionation of the four-phase assemblage plagioclase + olivine + clinopyroxene + orthopyroxene, but this is not considered plausible because orthopyroxene in the Concord gabbro is postcumulus, and probably was never of major importance in the crystallizing assemblage.

Each extraction diagram gives a range of proportions for each mineral in the crystallizing assemblage. Figure 12e illustrates the proportional ranges given by eight variation diagrams. This figure was constructed by determining the range of extract compositions given by each extraction diagram, and plotting each range on an equilateral plagioclase-olivine-clinopyroxene triangle. The area of overlap (shaded) is taken to be the range of mineral proportions in the assemblage most likely to produce the gabbro-syenite fractionation.

The validity of the fractionation assemblage of plagioclase + olivine + clinopyroxene was put to a more quantitative test using the least squares petrologic mixing calculations described by Wright and Doherty (1970). Average compositions of gabbro and syenite, and the same compositions of clinopyroxene and olivine used above were employed in the calculation. The plagioclase composition was allowed to "float"

between the most calcic (An 70) and the most sodic (An 39) observed values in the gabbro (analyses in Table 2). Addition of Fe-Ti oxides into the calculation resulted in an improved fit. The computed solution (Table 3) calls for removal of 95 weight % of a cumulate assemblage consisting of 57% plagioclase (An 62), 19% olivine, 18% clinopyroxene, 4% magnetite and 2% ilmenite from a melt of the average gabbro composition to produce a residual melt of the average syenite composition. The sum of the squares of the residuals (0.053) is low, and the error values are reasonable. The proportions of cumulus phases given by this method compare well with the values determined from major element extraction diagrams (Table 2).

Fractionation of Trace Elements

Trace element analyses for six gabbro samples and seven syenite samples (Price, 1969) are tabulated in Table A-12, in the Appendix. Figure 13 presents average trace element contents and standard deviations for gabbro and syenite versus the Differentiation Index (D.I. = normative Q + Or + Ab + Ne + Lc) of Thornton and Tuttle (1960). It is difficult to specify how fractionation affected these trace element contents because the concentrations in the original liquid are not precisely known. However, it seems likely that if the Concord gabbro is an early differentiate of the parent liquid, then the average Concord gabbro trace element content may be indicative of that of the parent magma.

In Figure 13, Zr and the alkalis K, Rb and Li are enriched in the syenite relative to the gabbro, whereas all other analyzed trace

Table 3. Solution to the Petrologic Mixing Problem

	Syenite	Olivine	Clinopyroxene	Magnetite	Ilmenite	Plagioclase	Observed Gabbro	Calculated Gabbro	Residual	Weight
SiO_2	61.86	37.71	51.16	0.00	0.00	52.78	47.74	47.62	0.10	1.00
Al_2O_3	17.40	0.00	3.21	0.81	0.10	30.10	17.90	17.86	0.04	1.00
FeO[a]	4.02	24.06	7.47	94.96	43.14	0.23	9.90	9.86	0.05	1.00
MgO	1.30	38.24	15.46	0.53	3.02	0.00	9.76	9.76	0.01	1.00
CaO	2.30	0.00	21.32	0.00	0.00	12.54	10.66	10.67	-0.01	1.00
Na_2O	7.58	0.00	0.56	0.00	0.00	4.17	2.56	2.75	-0.19	1.00
K_2O	4.49	0.00	0.00	0.00	0.00	0.21	0.32	0.34	-0.02	1.00
TiO_2	1.07	0.00	0.86	3.72	53.76	0.00	1.23	1.18	0.05	1.00
Total	100.02	100.01	100.04	100.02	100.02	100.03	100.05	100.04	$\sum r^2 = 0.0533$	
Solution	5.01	18.11	17.46	3.36	1.59	54.50(AN 52)				
Error[b]	1.1	0.3	0.7	0.1	0.2	0.7				
Composition of Cumulate Fraction[c]		19	18	4	2	57				

[a]Total Fe as FeO.

[b]Error estimated by empirical procedure of Wright and Doherty (1975).

[c]Composition of cumulate fraction recalculated to 100%.

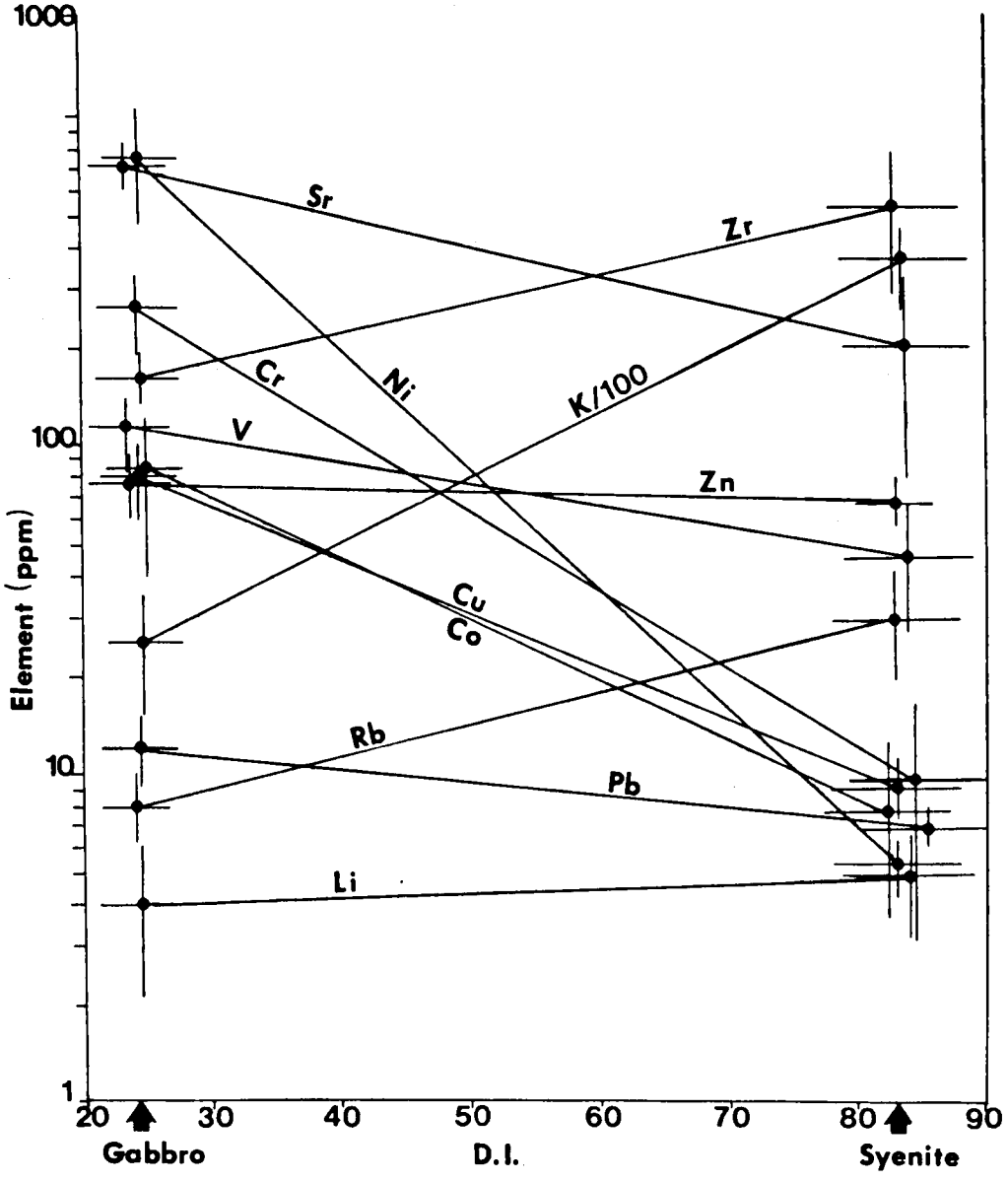

Figure 13. Trace element variations between average gabbro and syenite. These two rock types are separated by Differentiation Index. Vertical and horizontal bars represent 1 standard deviation.

elements are depleted. Fractionation of a spinel phase and a sulfide phase are suggested by depletion of Cr and V, and Cu and Zn, respectively. That a spinel phase was part of the fractionating assemblage required to produce syenitic magma is suggested from textural observations; magnetite and ilmenite occur as euhedral to subhedral inclusions in cumulus crystals. The bleb-shaped clusters of sulfide phases suggest an immiscible sulfide phase may have separated from the liquid at an early stage.

Two models describing the behavior of trace elements during fractional crystallization may be used to constrain the degree of fractional crystallization and the identity and proportions of crystallizing phases required to produce a particular residual magma (Arth, 1976). Rayleigh (or perfect) fractional crystallization assumes equilibrium between the surface of the crystallizing phases and the melt; this model may best describe rapidly cooled, shallowly emplaced magmas, where the cumulus phases are normally zoned. Equilibrium fractional crystallization assumes equilibrium between the total removed solid and the melt; this model is best applied to plutonic magmas, where cooling is slow enough to produce unzoned crystals which maintain equilibrium with the surrounding melt before fractionation.

The equations which describe the two crystallization models (e.g., McCarthy and Hasty, 1976) are:

(1) $\frac{C_l}{C_o} = F^{(D_a - 1)}$ for Rayleigh fractional crystallization, and

(2) $\frac{C_l}{C_o} = \frac{1}{F + D_a(1-F)}$ for equilibrium fractional crystallization,

where C_l is the concentration of trace element a in the residual melt, C_o is the concentration of a in the original melt, F is the weight fraction of melt remaining, and D_a is the bulk distribution coefficient for element a. D_a is obtained by:

$$D_a = \sum_i K_a^i x_i$$

where K_a^i is the distribution coefficient for element a in phase i, and x_i is the weight fraction of phase i in the fractionating assemblage.

The Rayleigh fractional crystallization equation produces a straight line on a logarithmic plot comparing two trace element concentrations, and the equilibrium fractional crystallization equation produces a curved line. In Figure 14, logarithmic plots of Rb versus Sr and Rb versus Zr in Concord gabbro and syenite are presented. Distribution coefficients for Rb, Sr and Zr for various phases (Arth, 1976; Cox et al., 1979; Pearce and Norry, 1979) depend on liquid composition; for these calculations an average value for silica (55%) intermediate between that for gabbro (48%) and syenite (61%) was chosen. In both Figures 14a and b, the gabbro-syenite trend coincides with the vector along which a melt fractionating plagioclase, olivine, clinopyroxene, and magnetite by Rayleigh fractional crystallization occurs. The least squares magma fractionation model indicated that 95% fractionation by weight of the given cumulus assemblage was required to produce a melt of average syenitic composition from the average gabbro composition. The vector lengths for Rayleigh fractionation in Figure 14a and b suggest degrees of fractionation of 85% and 80%, respectively, may be more

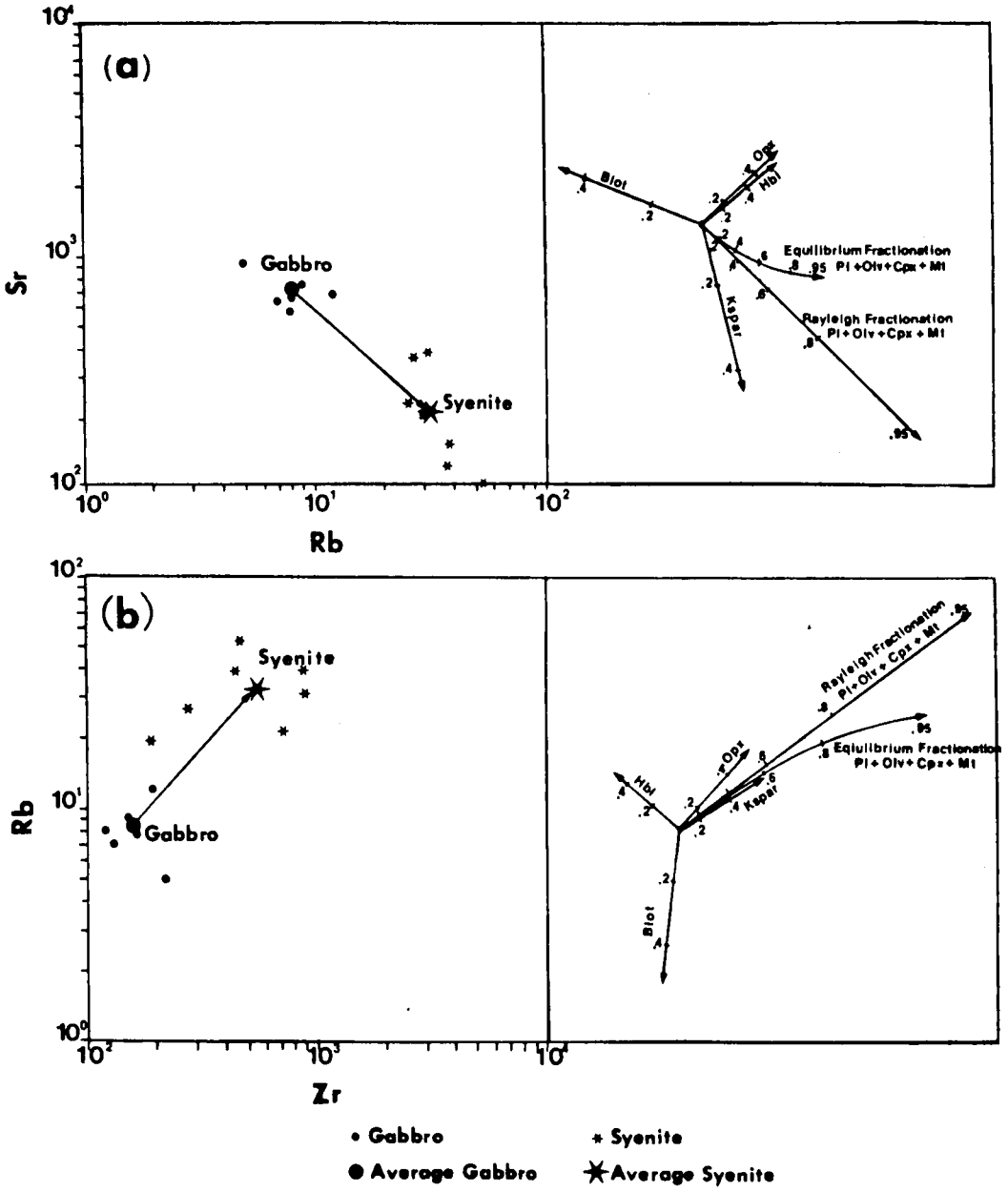

Figure 14. Rb-Sr (a) and Rb-Zr (b) variation diagrams (ppm) for Concord gabbro and syenite. The vectors in the upper right corners show the effects on average gabbro composition of crystallizing the assemblage Pl + Ol + Cpx + Mt in the proportions indicated by the petrologic mixing program, as well as other possible fractionating phases. Both Rayleigh fractionation and equilibrium fractionation trends are illustrated for the proposed fractionating assemblage.

appropriate for this fractionation model. However, the vector lengths are in good agreement with those calculated for major elements if fractionation is modeled as some combination of Rayleigh and equilibrium process (the latter produced shorter vectors at 95% fractionation). Although fractionation of a small amount of biotite can also explain this discrepancy, it does not appear necessary from these diagrams to fractionate any phases other than the given cumulus assemblage plag + cpx + ol + mt (+ ilm? + sulfide?) in order to produce syenite. Although a small amount of biotite fractionation is permitted, it seems unlikely because all biotite in the gabbro is postcumulus and syenite contains almost no biotite.

CHAPTER V

DISCUSSION

Inferences About the Parental Magma

If the average composition of the Concord gabbro is near the composition of the parental magma, then this magma was intermediate between a mildly alkaline basalt and a tholeiitic basalt. In variation diagrams in which various oxides are plotted against the Differentiation Index, the compositions of the Concord samples lie remarkably close to the line which represents extrusive alkali basalt-to-trachyte series from various localities (e.g. Poldervaart and Parker, 1964).

The Concord gabbro samples almost certainly represent cumulate rocks, so it is unlikely that whole rock analyses represent liquid compositions. This can be seen in Figure 12, p. 35, in which the norms of the analyzed gabbro samples do not fall within the fields of either alkaline or tholeiitic basalts. Fractionation of either olivine plus plagioclase or clinopyroxene plus plagioclase will have the effect of moving these samples along the Ol-Di join in this figure, along which many of them presently cluster. Therefore, the parental liquid must have been very close to this join, i.e. transitional between tholeiitic and milkly alkaline.

Petrogenesis

Geochemical evidence above suggests that the parental magma for the Concord gabbro and syenite was probably tholeiitic in composition,

or transitional between tholeiitic and alkali basalt. In other words, its composition plotted on or near the critical plane of silica-undersaturation on the normative basalt tetrahedron, defined by the plane Fo-Di-Ab. Based on the chronologic and spatial association of gabbro and syenite, and the plausible fractionation model relating these two rock types, it is concluded that the syenite is a late differentiation product of the gabbroic parental magma. Arguments already presented indicate that such a melt experienced fractionation of plagioclase, olivine and clinopyroxene in approximately cotectic proportions (fractionation of minor amounts of sulfide and Fe-Ti oxide minerals also occurred) in order to produce this syenitic end product.

Morse (1980), in a discussion of what he termed the "syenite problem," questioned the ability of a basaltic liquid with composition even slightly deviant from the critical plane to produce a trachytic liquid. In the system $NaAlSiO_4$-$KAlSiO_4$-SiO_2 (Figure 15a), a basalt of critical plane composition will fractionate to a trachytic liquid along the feldspar minimum, which is actually a narrow thermal maximum relative to the nepheline and silica minima (Figure 15b). Morse suggested that a slight deviation from the critical plane composition should cause the liquid to migrate down one of the steep liquidus slopes to either side of this thermal maximum, towards either the nepheline or silica thermal minimum, producing phonolitic or rhyolitic residual liquids, respectively. Although the parental magma for the Concord complex may have been of critical plane composition, it is difficult to imagine that all trachyte and syenite bodies owe their existence to fractionation along this precarious thermal divide.

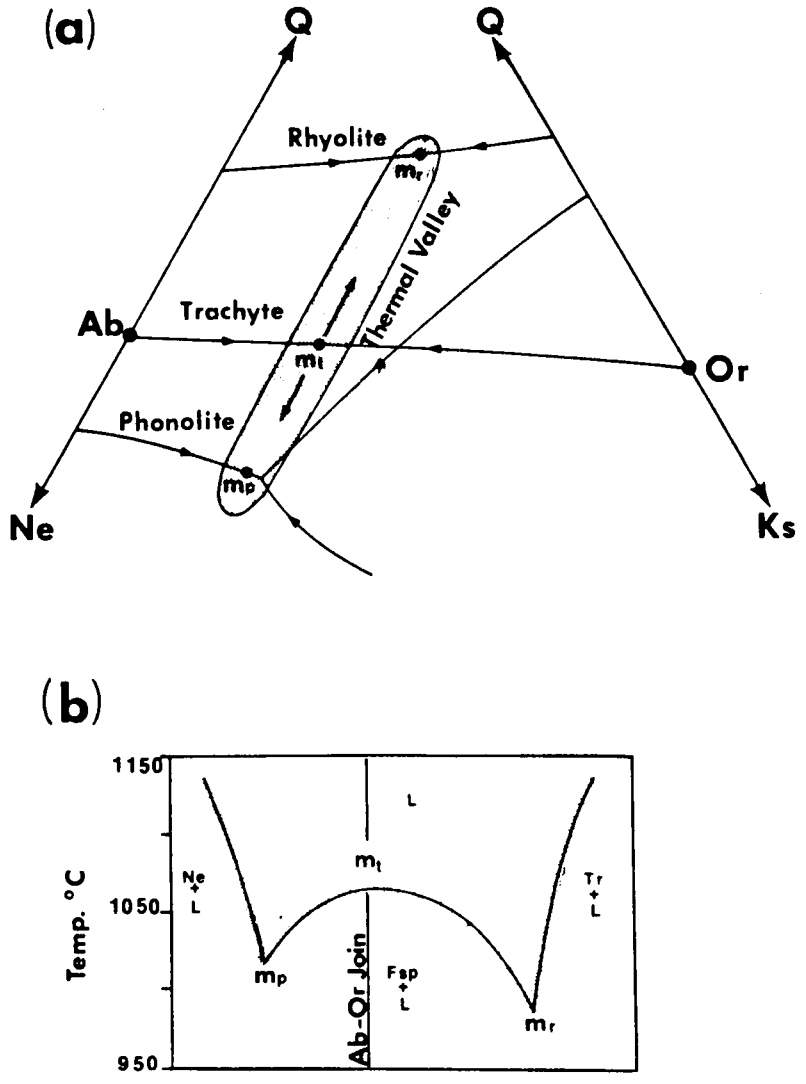

Figure 15. The thermal valley and profile along the thermal valley in Petrogeny's Residua System.

(a) The thermal "valley" in the system Ne-Ks-SiO_2 (Morse, 1980), encompassing three thermal minima: Mp (phonolite minimum), M_t (trachyte minimum) and M_r (rhyolite minimum).

(b) Profile along the thermal valley (Morse, 1980). Within this valley, the trachyte "minimum" M_t is actually a thermal maximum relative to Mp and M_r.

Cox et al. (1979) showed that while a basaltic liquid that is nepheline- or hypersthene-normative is expected to produce a phonolitic or rhyolitic residue, a liquid that is lying slightly to either side of the thermal divide would require a very large degree of crystallization to migrate to the compositions of these end-product liquids. Cox et al. observed that during this crystallization, the liquid becomes sufficiently enriched in alkalis to become trachytic long before a phonolitic or rhyolitic residue can be produced (Figure 16). This appears to support the suggestion by Morse (1980) that the feldspar join of Petrogeny's Residua System may be more accurately represented by a thermal "plateau" than by a sharp peak, which would allow for slight compositional deviations in fractionation of residual trachytic liquids. The Concord fractionation trend, therefore, apparently represents a tholeiitic or transitional basaltic liquid differentiating close to the critical plane of silica undersaturation to produce a syenitic melt with composition close to the feldspar join in the system Q-Ne-Ks.

The absence of any rocks of intermediate composition indicates that fractionation to form the syenitic liquid occurred at depth, followed by intrusion of this magma into a region of fracture between the gabbro body and the country rock. Similar bimodal distributions are common in extrusive basalt-trachyte provinces (e.g. Upton, 1974). One possible explanation for the missing intermediate rocks is given by Upton (1974) who suggested that intermediate liquids may be more viscous, i.e. less mobile, than basaltic liquids (which are hotter and less viscous) and syenitic liquids (with higher volatile contents).

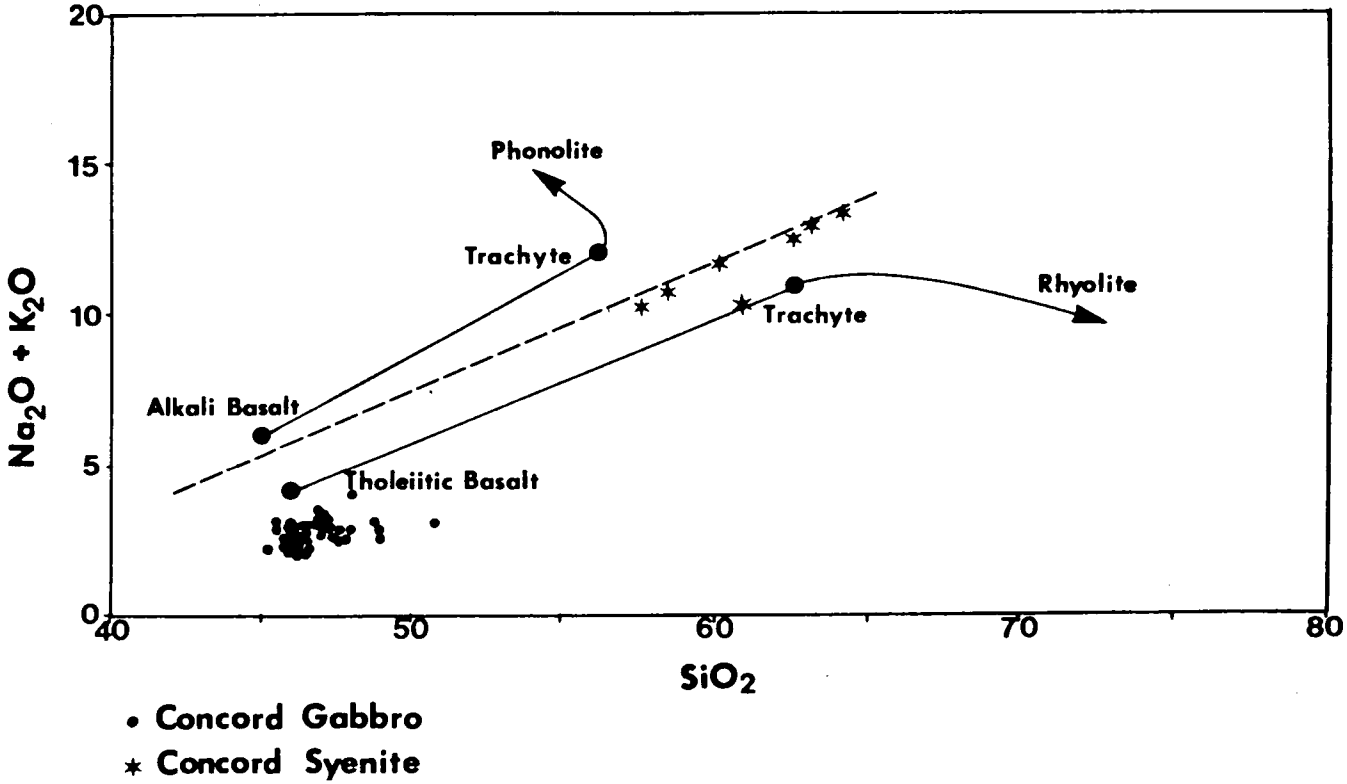

Figure 16. Total alkalis vs. silica (weight %) for Concord gabbro and syenite. Compositions plot near the projection of the plane of critical silica undersaturation, represented by the dashed line (Ol-Cpx-Pl at the basaltic end, Ab-Or at the trachytic end, after Cox et al., 1979). Basalts of compositions lying close to either side of this line (schematically represented by large dots) may fractionate to produce trachyte, before "falling off" this thermal divide towards phonolite or rhyolite.

Another possibility is that a fairly flat portion of the liquidus trajectory between the gabbro and syenite would cause a large degree of fractionation over a small temperature interval. In this situation, not many rocks of intermediate composition would be produced.

Conclusions

1. The Concord gabbro and syenite are associated spatially and temporally. This study establishes a possible petrogenetic relationship between the gabbro and syenite, using petrography, mineral compositions and bulk rock chemistry.

2. Geophysical modelling suggests the Concord complex consists of a 6 km-deep gabbro pluton surrounded by a steep-walled syenite ring dike, dipping outwardly at an angle of about 78° on the west side, with a vertical dip on the east side. This configuration probably resulted when the syenitic liquid intruded the fractured contact region between the gabbro body and the surrounding country rock.

3. Petrography and geochemical modelling suggest that production of the Concord syenite involved extensive fractional crystallization of olivine, plagioclase, and clinopyroxene, with minor sulfide and oxide minerals, from a basaltic parental magma at depth before intrusion to the present level.

4. The Concord trend probably represents near-critical plane differentiation of a tholeiitic or transitional basaltic liquid to a syenitic residual liquid with composition close to that of the alkali feldspar join in the system Q-Ne-Ks. Fractionation of the same mineral

assemblage from a range of basalt compositions should produce syenitic residua.

LIST OF REFERENCES

LIST OF REFERENCES

Albee, A. L. and L. Ray (1970) Correction factors for electron probe microanalysis of silicates, oxides, carbonates,phosphates, and sulfates. Anal. Chem., 42, 1408-1414.

Amber, E. P. and P. M. Ashley (1980) Mineralogy and petrology of the Dutchmans Creek gabbro intrusion, South Carolina: discussion. Am. Mineral., 65, 1302-1303.

Arth, J. G. (1976) Behavior of trace elements during magmatic processes—a summary of theoretical models and their applications. U.S.G.S. J. Research, 4, 41-47.

Bell, H. (1960) A synthesis of geologic work in the Concord Area, North Carolina. U.S.G.S. Professional Paper, 400B, 189-191.

Bence, A. E. and A. L. Albee (1968) Empirical correction factors for the electron microanalysis of silicates and oxides. J. Geol., 76, 382-403.

Butler, J. R. and P. C. Ragland (1969) A petrochemical survey of plutonic intrusions in the Piedmont, Southeastern Appalachians, U.S.A. Contrib. Mineral. Petrol., 24, 164-190.

Cabaup, J. (1969) Origin and differentiation of the gabbro in the Concord ring dike, North Carolina Piedmont. Unpublished M.S. Thesis, University of North Carolina at Chapel Hill.

Chalcraft, R. G. (1970) Petrography and geophysics of the Rock Hill gabbro pluton, York County, South Carolina. Southeastern Geol., 11, 153-171.

Clark, S. R. (1980) Petrology of the Bear Poplar and Barber mafic intrusions, North Carolina. Unpublished M.S. Thesis, The University of Tennessee, Knoxville.

Cox, K. G., J. D. Bell and R. J. Pankhurst (1979) The Interpretation of Igneous Rocks. Allen and Unwin, London.

Deer, W. A., R. A. Howie and J. Zussman (1966) An Introduction to the Rock-Forming Minerals. Wiley and Sons, New York.

Fullagar, P. D. (1971) Age and origin of plutonic intrusions in the Piedmont of Southeastern Appalachians. Geol. Soc. Am. Bull., 82, 2845-2862.

Heier, K. S. (1964) A geochemical comparison of the Blue Mountain (Ontario, Canada) and Stjernoy (Finnmark, North Norway) nepheline syenite. Norsk. Geol. Tidssker., 45, 41-52.

Hermes, O. D. (1968) Petrology of the Mecklenburg gabbro-metagabbro complex, North Carolina. Contrib. Mineral. Petrol., 18, 270-294.

Johnson, R. W. and R. G. Bates (1960) Aeromagnetic and aeroradioactivity survey of the Concord Quadrangle, North Carolina. U.S.G.S. Prof. Papers, 400B, 182-195.

Leake, B. E. (1978) Nomenclature of amphiboles. Am. Mineral., 63, 1023-1052.

McCallum, I. S., L. D. Raedeke, and E. A. Mathez (1980) Investigations of the Stillwater complex: part I: stratigraphy and structure of the Banded zone. Am. J. Sci., 280A, 59-87.

McCarthy, T. S. and R. A. Hasty (1976) Trace element distribution patterns and their relationship to the crystallization of granitic melts. Geochim. Cosmochim. Acta, 40, 1351-1358.

McSween, H. Y. (1980) Mineralogy and petrology of the Dutchmans Creek gabbroic intrusion, South Carolina: reply. Am. Mineral., 65, 1304-1306.

Medlin, J. H. (1968) Comparative petrology of two igneous complexes in the South Carolina Piedmont. Unpublished Ph.D. Thesis, Pennsylvania State University.

Morgan, B. A. (1963) A gravity survey of a ring-dike near Concord, North Carolina. Unpublished M.S. Thesis, University of North Carolina at Chapel Hill.

Morse, S. A. (1980) Basalts and Phase Diagrams. Springer-Verlag, New York.

Morse, S. A. and G. L. Davis (1968) Fractionation of potassium and rubidium in a layered intrusion. Carnegie Inst. Wash. Yearb., 67, 231-233.

Neilson, M. J. and G. F. Brockman (1977) The error associated with point counting. Am. Mineral., 62, 1238-1244.

Nockolds, S. R. (1964) Average chemical compositions of some igneous rocks. Geol. Soc. Amer. Bull., 65, 1007-1032.

Parsons, I. (1979) The Klokken gabbro-syenite complex, South Greenland: cryptic variation and origin of inversely graded layering. J. Petrol., 20, 653-694.

Pearce, J. A. and M. J. Norry (1979) Petrogenetic implications of Ti, Zr, Y, and Nb variations in volcanic rocks. Contrib. Mineral. Petrol., 69, 33-47.

Poldervaart, A. and A. B. Parker (1964) The Crystallization index as a parameter of igneous differentiation in binary variation diagrams. Am. J. Sci., 262, 281-289.

Price, V. (1969) Distribution of trace elements in plutonic rocks of the southeastern Piedmont. Ph.D. Thesis, University of North Carolina at Chapel Hill.

Shaw, D. M. (1968) A review of K-Rb fractionation trends by covariance analysis. Geochim. Cosmochim. Acta, 32, 573-601.

Streckeisen, A. L. (1973) Plutonic rocks—classification and nomenclature. Geotimes, 18, 43-63.

Talwani, M., J. L. Worzel, and M. Landisman (1959) Rapid gravity computations for two-dimensional bodies with application to the Mendocino submarine fracture zone. J. Geophys. Research, 64, 49-59.

Taylor, S. R. (1965) The application of trace element data to problems in petrology. In L. H. Ahrens, F. Press, S. K. Runcorn and H. C. Urey, Eds., Physics and Chemistry of the Earth, Pergamon, London.

Thornton, C. P. and O. F. Tuttle (1960) Chemistry of igneous rocks, I. Differentiation Index. Amer. J. Sci., 258, 664-684.

Upton, B. G. J. (1974) The alkaline province of south-west Greenland. In H. Sorensen, Ed., The Alkaline Rocks, Wiley and Sons, London, 221-38.

Van der Plas, L. and A. C. Tobi (1965) A chart for judging the reliability of point counting results. Am. J. Sci., 263, 87-90.

Wager, L. R., G. M. Brown and W. J. Wadsworth (1960) Types of igneous cumulates. J. Petrology, 1, 73-85.

Watson, T. L. and F. B. Laney (1906) The building and ornamental stones of North Carolina. N.C. Geol. Survey Bull., 2, 283 p.

Wilson, F. A. (1981) Geologic interpretation of geophysical data from the "Mecklenburg-Weddington" gabbro complex, southern Mecklenburg County, North Carolina. In J. W. Horton, Jr., J. R. Butler and D. M. Milton, Eds., Geological Investigations of the Kings Mountain Belt and Adjacent Areas in the Carolinas, South Carolina Geological Survey Columbia, 28-37.

Wright, T. L. and P. C. Doherty (1970) A linear programming and least squares computer method for solving petrologic mixing problems. Geol. Soc. Amer. Bull., 81, 1995-2008.

APPENDIX

Table A-1. Modal Variations: Concord Gabbro and Concord Syenite

	PLG	HBL	BIO	OPA	CPX	OPX	OLV	KSP	PRTH	QTZ	MON	APA	SERP	CHL	SER	ZIR	No. Points
									Concord Gabbro								
CG-4	64.1	5.5	0.4	1.4	16.1	10.9	-	-	-	-	-	0.7	0.4	0.3	0.2	-	1050
CG-5	56.8	2.5	4.6	6.9	15.8	12.1	-	-	-	-	-	0.4	0.1	0.7	0.1	-	1000
CG-6	69.5	7.1	0.6	2.7	5.5	7.9	5.0	-	-	-	-	0.2	0.4	0.7	0.3	0.1	1033
CG-9	52.1	24.7	0.9	5.9	0.7	10.3	2.7	-	-	-	-	0.6	-	1.9	0.2	-	1125
CG-10a	51.3	29.6	-	2.2	5.1	7.2	3.0	-	-	-	--	-	-	0.9	0.7	-	1147
CG-10b	46.9	26.3	-	1.1	18.5	5.8	-	-	-	-	-	0.4	0.4	0.2	0.4	-	1093
CG-11	61.6	5.0	-	4.3	12.8	14.0	1.0	-	-	-	-	0.3	0.3	0.6	0.1	-	1007
CG-22	45.2	36.6	-	6.5	0.6	4.5	0.1	-	-	-	-	0.7	0.1	2.8	2.9	-	1106
CG-23	52.1	30.3	0.1	2.5	3.0	8.8	0.9	-	-	-	-	0.4	-	1.8	-	0.1	1000
CG-25	57.3	24.1	0.2	3.0	1.8	9.6	3.0	-	-	-	-	0.3	0.1	0.3	0.3	-	1099
CG-26	47.2	33.3	0.1	3.3	2.7	10.8	1.5	-	-	-	-	-	-	0.5	0.6	-	1072
CG-27	58.9	11.7	-	1.9	0.1	13.8	12.4	-	-	-	-	0.3	0.2	0.2	0.5	-	1122
CG-33	59.3	20.2	3.1	2.4	2.2	9.1	1.7	-	-	-	-	-	0.2	1.6	0.2	-	1059
CG-47	46.2	36.8	0.4	3.2	0.7	11.8	-	-	-	-	-	0.2	-	0.4	0.3	-	1048
CG-50	68.9	4.0	-	2.3	3.0	3.6	16.1	-	-	-	-	0.1	0.5	0.5	1.0	-	1129
CG-53	62.8	5.6	1.5	2.2	2.9	10.5	13.4	-	-	-	-	0.2	0.4	0.1	0.4	-	1000
CG-54	47.5	16.7	1.6	4.5	2.6	11.4	14.6	-	-	-	-	0.2	-	0.4	0.5	-	1160
CG-57	65.3	8.0	2.3	3.5	0.8	12.8	6.2	-	-	-	-	0.3	-	0.5	0.3	-	1141
CG-58	65.8	3.7	1.3	3.2	12.9	7.4	4.9	-	-	-	-	-	0.1	0.5	0.2	-	1181
CG-73	62.4	1.9	1.7	4.0	14.2	7.2	7.4	-	-	-	-	-	0.1	0.2	0.9	-	1128
CG-74	64.9	7.3	3.1	5.6	10.2	6.9	0.9	-	-	-	-	0.2	0.4	0.3	0.2	-	1105
CG-81	58.5	7.9	4.0	5.2	12.2	11.8	-	-	-	-	-	0.3	-	0.1	-	-	1088

Table A-1 (continued)

	PLG	HBL	BIO	OPA	CPX	OPX	OLV	KSP	PRTH	QTZ	MON	APA	SERP	CHL	SER	ZIR	No. Points
CG-84	65.5	3.4	-	5.5	6.0	15.3	3.5	-	-	-	-	0.3	0.1	0.3	-	0.1	1102
CG-87	64.5	14.7	-	4.4	1.0	10.8	2.7	-	-	-	-	0.1	0.2	0.8	0.6	0.2	1000
CG-90	64.5	10.4	1.6	2.8	0.2	13.7	5.1	-	-	-	-	0.2	-	1.2	0.3	-	1000
CG-92	62.2	15.8	1.5	2.7	6.6	7.7	2.9	-	-	-	-	-	-	0.4	0.2	-	1085
CG-98	58.4	4.2	-	8.2	10.8	11.2	6.4	-	-	-	-	-	0.4	0.4	-	-	1151
CG-102	50.6	17.6	-	3.5	12.2	10.7	4.7	-	-	-	-	-	0.1	0.3	0.3	-	1062
CG-104	53.0	25.8	2.0	2.4	0.4	15.0	0.4	-	-	-	-	0.3	0.5	-	0.2	-	1200
CG-105	51.0	21.3	-	2.3	8.9	15.7	-	-	-	-	-	0.3	-	0.4	0.1	-	1172
CG-106a	53.9	16.2	-	3.9	14.9	10.5	-	-	-	-	-	0.4	-	0.1	0.1	-	1097
CG-106b	54.3	24.4	-	5.2	4.7	10.5	-	-	-	-	-	0.4	-	0.5	-	-	1136
CG-107	51.8	23.7	-	6.5	17.7	8.9	-	-	-	-	-	0.2	0.1	0.6	0.5	-	1117
								Concord Syenite									
CS-39	4.3	1.3	0.2	2.6	2.6	-	-	3.4	82.4	2.6	0.6	-	-	-	-	-	621
CS-62	4.8	3.1	0.2	2.9	4.2	-	-	3.1	77.0	4.0	0.4	0.4	-	-	-	-	523
CS-88	3.2	-	-	-	-	-	-	3.2	57.0	36.1	-	-	-	-	-	0.4	554
CS-2	0.5	0.4	0.4	2.9	5.1	-	-	0.5	86.6	0.7	1.1	0.9	-	-	-	0.9	553
CS-37	18.6	-	1.8	1.8	2.7	-	-	1.8	68.5	3.9	0.4	0.6	-	-	-	-	515
CS-20a	4.8	1.0	0.6	3.0	4.2	-	-	1.5	79.8	3.2	1.0	0.8	-	-	-	0.2	524

Table A-2. Representative Electron Microprobe Analyses: Plagioclase

	CG-50[7]	CG-33 [5]	CG-9 [4]	CG-5 [9]	CG-10 [8]	CG-73 [4]	CS-43 [14]	CS-51 [10]	CS-12 [5]
SiO_2	51.4 (6)	53.9 (3)	50.0 (10)	59.1 (10)	53.8 (3)	52.8 (5)	68.2 (4)	69.5 (4)	65.1 (3)
Al_2O_3	31.1 (4)	29.2 (4)	31.4 (7)	25.2 (6)	29.0 (3)	30.4 (3)	20.1 (2)	19.2 (1)	21.4 (1)
FeO*	0.20(3)	0.16(5)	0.23(5)	0.21(4)	0.26(5)	0.32(5)	0.16(8)	0.29(12)	0.29(21)
CaO	12.8 (7)	11.2 (5)	14.0 (10)	7.63(99)	11.7 (3)	12.2 (3)	0.86(7)	0.26(9)	2.77(10)
Na_2O	4.02(41)	4.87(35)	3.29(52)	6.61(69)	4.39(32)	3.97(15)	11.0 (2)	11.2 (3)	9.63(29)
K_2O	0.13(2)	0.25(4)	0.08(3)	0.57(13)	0.17(2)	0.19(2)	0.10(2)	0.20(18)	0.27(22)
Total	99.67	99.50	99.03	99.29	99.30	99.83	100.46	100.60	99.46
					Cations/8 Oxygens				
Si	2.341	2.444	2.300	2.657	2.444	2.390	2.967	3.013	2.877
Al	1.667	1.558	1.701	1.336	1.551	1.626	1.032	0.982	1.117
Fe	0.006	0.005	0.008	0.008	0.009	0.012	0.005	0.010	0.010
Ca	0.622	0.542	0.691	0.367	0.572	0.588	0.040	0.011	0.131
Na	0.354	0.427	0.292	0.575	0.387	0.348	0.926	0.936	0.826
K	0.006	0.013	0.004	0.031	0.009	0.010	0.005	0.010	0.014
Total	4.997	4.989	4.996	4.974	4.973	4.971	4.975	4.965	4.975

[a] CG is Concord gabbro, CS is Concord Syenite. Unit in [ ] is the number of replicate analyses averaged.

[b] Units in ( ) represent one standard deviation in terms of least units cited.

[c] Values in weight % oxides.

*All Fe reported as FeO.

Table A-3. Representative Electron Microprobe Analyses: Bulk Perthite

	CS-43 [7]	CS-12 [6]	CS-51 [19]
SiO_2	66.3 (5)	66.5 (3)	65.7 (3)
Al_2O_3	19.8 (1)	20.5 (1)	18.5 (2)
FeO*	0.14(5)	0.09(3)	0.47(11)
CaO	0.17(10)	1.89(17)	-
Na_2O	4.59(261)	7.79(116)	3.87(218)
K_2O	10.0 (40)	3.30(189)	10.6 (32)
Total	100.08	100.04	99.12
		Cations/8 Oxygens	
Si	2.996	2.937	3.002
Al	1.000	1.067	0.995
Fe	0.005	0.002	0.017
Ca	0.008	0.089	-
Na	0.401	0.667	0.342
K	0.576	0.185	0.617
Total	4.986	4.947	4.973

[a]CS is Concord syenite. Unit in [ ] is the number of replicate analyses averaged.

[b]Values in weight % oxides. Units in ( ) represent one standard deviation in terms of least units cited.

*All Fe reported as FeO.

Table A-4. Representative Electron Microprobe Analyses: Orthopyroxene

	CG-33 [7]	CG-9 [8]	CG-50 [4]	CG-73 [6]
SiO_2	53.8 (2)	54.4 (2)	55.4 (3)	53.7 (2)
TiO_2	0.08(1)	0.12(1)	0.16(3)	0.32(1)
Al_2O_3	1.38(4)	1.49(5)	1.77(5)	1.47(6)
FeO*	16.4 (1)	15.6 (2)	13.1 (2)	15.7 (2)
MnO	0.48(2)	0.41(3)	0.40(2)	0.57(3)
MgO	26.5 (2)	27.6 (1)	30.0 (1)	26.6 (2)
CaO	1.00(8)	0.82(11)	0.59(9)	1.07(8)
Na_2O	0.03(1)	0.03(2)	0.07(1)	0.07(1)
Total	99.72	100.38	101.52	99.64
		Cations/6 Oxygens		
Si	1.958	1.953	1.948	1.952
Ti	0.002	0.003	0.004	0.008
Al	0.059	0.062	0.073	0.063
Fe	0.500	0.467	0.384	0.476
Mn	0.014	0.011	0.010	0.017
Mg	1.437	1.475	1.571	1.443
Ca	0.038	0.030	0.021	0.040
Na	0.002	0.002	0.004	0.004
Total	4.010	4.003	4.015	4.003

[a]CG is Concord gabbro, CS is Concord syenite. Unit in [ ] is the number of replicate analyses averaged.

[b]Values in weight % oxides. Units in ( ) represent one standard deviation in terms of least units cited.

*All Fe reported as FeO.

Table A-5. Representative Electron Microprobe Analyses: Clinopyroxene

	CG-33 [3]	CG-50 [6]	CG-5 [6]	CG-10 [5]	CS-12 [5]	CS-43 [4]	CS-51 [5]
SiO_2	52.4 (4)	51.3 (6)	50.9 (7)	51.3 (3)	53.1 (2)	53.2 (3)	53.7 (2)
TiO_2	0.52(9)	1.03(21)	0.77(16)	0.59(3)	0.59(15)	0.37(9)	0.21(1)
Al_2O_3	3.14(20)	3.76(34)	2.50(28)	2.29(11)	1.36(6)	0.68(5)	0.64(3)
FeO*	7.36(14)	6.71(50)	7.60(33)	8.51(20)	8.70(27)	8.80(21)	10.4 (2)
MnO	0.46(4)	0.14(1)	0.51(4)	0.37(4)	1.32(2)	1.41(3)	1.87(12)
MgO	14.9 (2)	15.6 (3)	15.3 (2)	15.0 (1)	15.1 (2)	13.2 (1)	12.2 (1)
CaO	21.7 (1)	21.3 (6)	21.3 (5)	21.1 (2)	19.4 (2)	20.6 (1)	19.8 (1)
Na_2O	0.47(3)	0.52(10)	0.67(3)	0.50(2)	0.69(3)	1.26(8)	1.43(5)
Total	100.95	100.36	99.66	99.72	100.26	99.55	100.20
				Cations/6 Oxygens			
Si	1.926	1.888	1.902	1.917	1.969	1.997	2.013
Ti	0.014	0.028	0.021	0.016	0.016	0.010	0.005
Al	0.136	0.163	0.109	0.100	0.059	0.029	0.027
Fe	0.225	0.206	0.236	0.265	0.269	0.275	0.326
Mn	0.014	0.003	0.015	0.011	0.041	0.044	0.059
Mg	0.815	0.854	0.854	0.833	0.832	0.740	0.681
Ca	0.853	0.839	0.853	0.845	0.770	0.828	0.794
Na	0.033	0.037	0.048	0.035	0.049	0.091	0.103
Total	4.016	4.018	4.038	4.022	4.005	4.014	4.008

[a] CG is Concord gabbro, CS is Concord syenite. Unit in [ ] is the number of replicate analyses averaged.

[b] Units in ( ) represent one standard deviation in terms of least units cited.

[c] Values in weight % oxides.

*All Fe reported as FeO.

Table A-6. Representative Electron Microprobe Analyses: Olivine

	CG-33 [6]	CG-9 [8]	CG-50 [4]	CG-73 [4]
SiO_2	37.3 (1)	37.4 (1)	37.9 (1)	37.8 (2)
FeO*	24.7 (2)	26.5 (2)	21.2 (1)	23.6 (1)
MnO	0.51(3)	0.50(4)	0.41(4)	0.57(3)
MgO	36.4 (2)	35.4 (2)	41.2 (1)	38.1 (1)
NiO	0.17(2)	n.a.	n.a.	n.a.
Total	99.08	99.80	100.71	100.07
		Cations/4 Oxygens		
Si	0.995	0.996	0.976	0.989
Fe	0.550	0.591	0.457	0.516
Mn	0.011	0.011	0.008	0.012
Mg	1.446	1.404	1.579	1.489
Ni	0.003	-	-	-
Total	3.005	3.002	3.020	3.006

[a]CG is Concord Gabbro, CS is Concord syenite. Unit in [ ] is the number of replicate analyses averaged.

[b]Values in weight % oxides. Units in ( ) represent one standard deviation in terms of least units cited.

*All Fe reported as FeO.

n.a. = Oxide not analyzed.

Table A-7. Representative Electron Microprobe Analyses: Amphibole

	CG-33 [4]	CG-9 [4]	CG-50 [3]	CG-73 [4]	CG-10 [4]	CS-43 [6]	CS-51 [5]
SiO_2	41.0 (1)	41.2 (1)	41.6 (1)	41.5 (1)	41.9 (3)	49.6 (3)	50.8 (2)
TiO_2	2.91(12)	3.89(13)	3.15(7)	4.04(7)	3.91(4)	1.28(11)	0.92(4)
Al_2O_3	12.4 (2)	11.2 (1)	11.9 (1)	11.9 (1)	11.4 (1)	3.93(4)	3.09(1)
Fe_2O_3*	2.40	3.77	4.70	1.70	2.57	10.3	9.34
FeO	8.66(21)	8.33(20)	4.95(21)	9.63(23)	10.2 (3)	3.58(23)	3.15(9)
MnO	0.22(4)	0.22(3)	0.18(3)	0.21(2)	0.19(5)	1.50(9)	1.76(7)
MgO	13.5 (2)	13.5 (1)	15.6 (2)	13.3 (1)	12.9 (1)	16.1 (2)	16.7 (1)
CaO	11.5 (6)	11.2 (1)	11.8 (2)	11.5 (1)	11.6 (1)	10.3 (3)	9.84(12)
Na_2O	2.47(2)	2.50(5)	2.64(9)	2.41(11)	2.24(5)	1.93(14)	2.41(9)
K_2O	1.17(2)	1.02(6)	0.84(1)	1.13(5)	0.95(6)	0.56(4)	0.67(2)
Total	96.16	96.86	97.29	97.24	97.84	99.12	98.75
				Cations/23 (O, OH, F)			
Si	6.125	6.127	6.072	6.139	6.182	7.076	7.297
Ti	0.327	0.435	0.356	0.450	0.434	0.137	0.068
Al	2.173	1.961	2.048	2.073	1.988	0.660	0.475
Fe^{3+}	0.270	0.422	0.516	0.189	0.285	1.109	1.067
Fe^{2+}	1.082	1.035	0.604	1.192	1.295	0.427	0.381
Mn	0.028	0.028	0.022	0.026	0.024	0.181	0.261
Mg	2.996	2.993	3.393	2.932	2.828	3.411	3.451
Ca	1.848	1.785	1.840	1.821	1.831	1.576	1.507
Na	0.716	0.720	0.747	0.692	0.641	0.534	0.596
K	0.223	0.193	0.156	0.213	0.179	0.102	0.109
Total	15.789	15.698	15.747	15.727	15.651	15.214	15.211

[a] CG is Concord gabbro, CS is Concord syenite. Unit in [ ] is the number of replicate analyses averaged.

[b] Values in weight % oxides. Units in ( ) represent one standard deviation in terms of least units cited.

*All Fe is determined as FeO, Fe^{3+} calculated by stoichiometry.

Table A-8. Representative Electron Microprobe Analyses: Biotite

	CG-9 [4]	CG-33 [4]	CG-5 [4]	CG-73 [4]	CS-51 [5]	CS-12 [5]
SiO_2	35.9 (2)	36.6 (1)	37.4 (11)	37.6 (3)	40.4 (4)	38.9 (6)
TiO_2	5.41(3)	4.96(2)	6.84(14)	3.76(25)	2.10(15)	5.11(9)
Al_2O_3	15.4 (1)	14.9 (1)	14.1 (1)	16.4 (5)	11.5 (2)	12.8 (2)
FeO*	9.34(26)	10.2 (2)	11.4 (2)	7.90(50)	12.9 (5)	14.3 (2)
MnO	0.11(2)	0.06(3)	0.05(4)	-	0.61(8)	0.35(4)
MgO	17.6 (2)	17.1 (2)	15.5 (2)	19.2 (7)	18.1 (3)	16.0 (2)
Na_2O	0.53(2)	0.50(2)	0.20(4)	0.59(14)	0.09(1)	0.14(3)
K_2O	8.59(18)	8.45(8)	9.55(6)	8.73(62)	9.12(20)	9.05(29)
Total	92.88	92.83	95.08	94.23	94.76	96.58
			Cations/11 (O, OH, F)			
Si	2.682	2.740	2.762	2.735	2.991	2.850
Ti	0.302	0.279	0.376	0.205	0.115	0.280
Al	1.358	1.313	1.229	1.407	1.000	1.108
Fe	0.583	0.637	0.699	0.479	0.798	0.874
Mn	0.006	0.002	0.002	-	0.037	0.021
Mg	1.952	1.906	1.706	2.077	1.999	1.743
Na	0.074	0.070	0.028	0.081	0.013	0.019
K	0.817	0.806	0.898	0.808	0.861	0.846
Total	7.774	7.753	7.700	7.792	7.814	7.741

[a]CG is Concord gabbro, CS is Concord syenite. Unit in [ ] is the number of replicate analyses averaged.

[b]Units in ( ) represent one standard deviation in terms of least units cited.

[c]Values in weight % oxides.

*All Fe reported as FeO.

Table A-9. Representative Electron Microprobe Analyses: Oxides

	Pleonaste [3]	Magnetite [3]	Ilmenite [5]
TiO_2	0.13(20)	1.06(5)	51.9 (7)
Al_2O_3	62.6 (11)	0.65(5)	0.09(1)
Cr_2O_3	0.19(10)	0.28(2)	0.02(2)
Fe_2O_3*	4.68	58.6	4.82
FeO	18.8 (6)	39.9 (8)	37.5 (2)
MnO	0.21(5)	0.14(2)	3.13(9)
MgO	14.6 (4)	0.37(1)	2.91(8)
Total	100.52	101.06	100.39
Cation Basis	4	4	3
Ti	0.003	0.031	0.960
Al	1.922	0.028	0.002
Cr	0.004	0.008	-
Fe^{3+}	0.092	1.709	0.089
Fe^{2+}	0.395	1.294	0.771
Mn	0.005	0.005	0.065
Mg	0.569	0.021	0.107
Total	2.990	3.096	1.995

[a]All oxide analyses from sample CG-5. Unit in [ ] is the number of replicate analyses averaged.

[b]Values in weight % oxides. Units in ( ) represent one standard deviation in terms of least units cited.

*All Fe is determined as FeO, Fe^3 calculated by stoichiometry.

Table A-10. Bulk Chemical Compositions: Gabbro

	SiO_2	Al_2O_3	TiO_2	FeO*	MgO	CaO	Na_2O	K_2O	MnO	Total
1	46.4	17.22	1.27	10.15	10.96	10.31	2.49	0.40	0.14	99.34
2	45.9	12.96	1.89	11.48	17.47	9.03	1.87	0.32	0.16	101.08
3	46.5	17.14	1.31	9.57	8.27	11.67	2.56	0.16	0.15	97.33
5	46.6	15.50	0.94	11.52	11.85	10.54	2.12	0.10	0.15	99.32
6	45.8	18.41	0.54	9.91	12.14	9.59	2.44	0.12	0.13	99.08
8	47.6	17.52	1.17	9.17	7.96	12.27	2.45	0.20	0.13	98.47
9	48.8	18.18	0.92	7.05	7.59	13.01	2.45	0.11	0.12	98.23
10	45.9	18.28	0.80	8.98	9.65	10.96	2.35	0.12	0.13	97.17
11	46.8	17.59	1.69	10.06	7.36	10.31	2.97	0.42	0.17	97.37
13	46.4	17.92	0.99	9.34	9.96	10.32	2.53	0.36	0.13	97.95
14a	46.3	17.31	1.43	10.76	8.19	11.02	2.48	0.15	0.15	97.79
14c	47.4	18.77	1.10	8.68	7.54	11.54	2.53	0.13	0.13	97.82
14d	47.3	18.09	1.46	9.94	8.24	10.71	2.74	0.23	0.13	98.84
15	46.9	18.33	1.47	9.95	7.69	10.23	2.86	0.38	0.13	97.94
16	46.5	17.25	1.49	9.66	10.46	10.20	2.39	0.42	0.13	98.50
17	47.0	16.95	1.30	9.40	9.12	11.68	2.49	0.36	0.12	98.42
19	46.5	17.52	1.65	10.29	8.26	10.54	2.67	0.34	0.14	97.91
20	46.9	17.99	1.47	10.13	9.25	10.10	2.60	0.36	0.12	98.92
21	45.6	18.46	1.51	10.01	7.89	10.70	2.60	0.36	0.15	97.28
23	46.9	15.40	1.80	12.00	9.75	9.46	2.48	0.35	0.18	98.32
24	46.1	15.67	1.53	11.89	12.70	9.44	2.40	0.36	0.18	100.27
27a	47.6	17.37	1.14	8.83	8.34	11.54	2.45	0.31	0.13	97.71
27b	45.4	16.37	1.39	10.72	11.02	9.95	2.48	0.44	0.16	97.93
28	46.1	19.73	0.80	8.68	11.34	11.02	2.24	0.20	0.12	100.23
30	46.4	19.77	0.56	8.43	11.21	11.11	2.04	0.08	0.12	99.72
31	46.3	18.14	0.91	9.38	9.35	10.42	2.61	0.16	0.17	97.44
32	46.1	18.89	1.01	8.71	8.32	10.96	2.56	0.27	0.12	96.94
33	47.9	18.52	0.86	8.89	8.17	10.77	2.49	0.23	0.10	97.96
35	46.9	18.41	1.48	10.08	7.64	9.90	2.75	0.49	0.13	97.78
36	47.0	18.35	1.43	9.91	8.46	9.87	2.74	0.54	0.15	98.45
37	45.2	17.42	1.52	9.91	11.77	11.46	1.97	0.19	0.18	99.62
42	47.5	14.78	1.66	12.47	9.05	11.35	2.18	0.29	-	99.28
43	47.3	15.69	1.40	11.52	9.68	9.75	2.55	0.36	0.19	98.46
48	45.9	18.63	0.90	8.74	9.60	10.59	2.39	0.19	0.12	97.06
49	45.7	17.10	1.02	10.57	10.93	10.66	2.06	0.21	0.15	98.45
50	46.3	19.69	0.75	8.36	9.52	10.58	2.32	0.22	0.10	97.84
52	46.4	16.44	1.32	11.27	11.82	9.70	2.41	0.35	0.15	99.86
53	47.5	18.16	1.35	9.13	7.36	10.46	2.79	0.41	0.13	97.29
54	46.5	19.51	1.34	9.33	9.20	10.10	2.84	0.45	0.13	99.30
56	48.2	17.33	1.38	9.80	6.61	9.90	3.10	0.85	0.16	97.85
CRD-24	47.9	16.3	1.48	10.26	8.30	8.97	3.18	0.71	0.18	97.28
CRD-29	45.8	16.8	1.21	10.62	11.37	8.83	2.74	0.30	0.17	97.84
NC-3	50.7	17.5	0.72	7.46	8.83	10.66	2.71	0.18	0.12	98.88
NC-4	48.8	20.5	0.42	6.82	9.00	10.31	2.58	0.20	0.11	98.74
NC-16	48.8	19.6	0.58	6.69	8.25	10.86	2.70	0.28	0.11	97.87
NC-17	47.7	15.6	0.62	11.16	13.71	8.15	2.20	0.17	0.18	99.49

[a]Bulk chemical analyses 1-56 by Cabaup (1969), analyses CRD-24—NC-17 by Butler and Ragland (1969).

[b]All values are in weight % oxide.

*All Fe reported as FeO.

Table A-11. Bulk Chemical Compositions: Syenite

	SiO_2	Al_2O_3	TiO_2	FeO*	MgO	CaO	Na_2O	K_2O	MnO	Total
CRD-18	62.5	17.0	0.87	3.51	0.78	1.34	7.71	4.97	0.18	98.86
CRD-20	63.8	16.9	0.58	2.38	0.36	0.50	7.60	5.92	0.24	98.28
CRD-22	57.5	17.9	1.34	5.22	1.79	4.27	8.22	2.07	0.17	98.48
NC-28a	60.7	16.9	1.34	5.03	2.29	2.97	6.68	3.63	0.19	99.73
NC-140	58.3	17.5	1.20	4.71	1.52	2.94	6.88	3.94	0.20	97.19
NC-141	59.9	16.6	1.29	4.19	1.50	2.60	7.75	4.64	0.17	98.64
NC-142	62.8	17.1	0.73	2.64	0.68	1.21	7.32	5.73	0.16	98.37

[a]Bulk chemical analyses by Butler and Ragland (1969).

[b]All values are in weight % oxide.

*All Fe reported as FeO.

Table A-12. Trace Element Compositions

	Cu	Pb	Zn	Li	V	Cr	Co	Ni	Sr	Zr	Rb
CRD-24	76	12	88	7	181	144	29	240	690	189	12
CRD-19	64	11	97	6	110	195	110	780	586	157	8
NC-3	115	10	65	3	94	325	96	970	664	118	8
NC-4	58	9	62	2	96	295	32	680	935	216	5
NC-16	74	11	62	3	108	365	120	1180	756	155	9
NC-17	106	17	100	3	104	273	130	620	630	129	7
CRD-18	7	7	61	5	31	4	6	4	155	440	38
CRD-20	6	7	45	7	20	9	7	4	34	458	52
CRD-22	8	7	73	4	59	1	10	6	77	193	13
NC-28a	13	7	78	6	55	23	360	8	369	275	27
NC-140	10	7	86	6	69	15	7	4	384	895	31
NC-141	10	9	82	8	69	8	20	6	297	794	22
NC-142	6	7	54	2	29	8	11	4	124	882	37

[a]Analyses for trace elements by Price (1969). Samples CRD-24, 29, and NC-3, 4, 16, 17 are Concord gabbro, samples CRD-18, 20, 22, and NC-28a, 140, 141, 142 are Concord syenite.

[b]All values reported as ppm.

Table A-13. Normative Mineralogy

	Orthoclase	Albite	Anorthite	Nepheline	Na-Metasilicate	Diopside	(WO)	(EN)	(FS)	Hypersthene	(EN)	(FS)	Acmite	Olivine	(FO)	(FA)	Magnetite	Ilmenite	Total
1	2.35	20.26	34.84	0.51		13.38	6.94	4.66	1.77	-	-	-		22.59	15.98	6.61	3.62	2.43	99.98
2	1.87	15.65	25.74	-		14.81	7.75	5.64	1.42	3.46	2.77	0.69		30.91	24.27	6.64	4.02	3.55	100.01
3	0.97	22.25	35.75	-		19.19	9.90	6.34	2.95	0.60	0.41	0.19		15.20	10.09	5.11	3.47	2.56	99.99
6	0.72	20.74	39.29	0.05		7.02	3.64	2.46	0.91	-	-	-		27.61	19.66	7.96	3.54	1.03	100.00
8	1.20	21.01	36.70	-		20.21	10.43	6.69	3.09	3.52	2.42	1.10		11.55	7.69	3.86	3.56	2.25	100.00
9	0.66	21.10	38.96	-		21.51	11.16	7.51	2.84	6.61	4.81	1.80		6.85	4.85	2.00	2.54	1.78	100.01
10	0.73	20.46	40.10	-		12.77	6.61	4.39	1.77	2.12	1.51	0.60		18.99	13.19	5.80	3.27	1.56	100.00
11	2.55	25.80	34.32	-		14.77	7.60	4.71	2.46	0.55	0.23	0.12		15.26	9.72	5.54	3.65	3.30	100.00
13	2.17	21.85	37.23	-		12.10	6.27	4.18	1.65	0.55	0.40	0.16		20.79	14.53	6.26	3.37	1.92	99.98
14a	0.91	21.03	36.71	-		15.61	8.02	4.96	2.63	5.47	3.59	1.88		13.61	8.63	4.98	3.89	2.78	100.01
14c	0.79	21.88	40.35	-		14.70	7.58	4.84	2.28	6.54	4.47	2.08		10.47	6.92	3.54	3.14	2.14	100.01
14d	1.37	23.45	36.81	-		13.72	7.07	4.51	2.14	3.69	2.51	1.18		14.61	9.63	4.98	3.55	2.81	100.01
15	2.29	24.70	36.81	-		12.17	6.26	3.92	1.99	2.05	1.37	0.69		15.53	10.00	5.53	3.60	2.85	100.00
16	2.52	20.53	35.63	-		12.65	6.57	4.47	1.60	3.28	2.42	0.86		19.05	13.70	5.35	3.47	2.87	100.00
17	2.16	21.13	34.56	0.15		19.41	10.05	6.64	2.73	-	-	-		16.69	11.53	5.17	3.37	2.51	99.98
19	2.05	23.07	35.55	-		14.45	7.45	4.73	2.27	2.19	1.49	0.70		15.77	10.36	5.41	3.72	3.20	100.00
20	2.15	22.24	36.75	-		11.22	5.80	3.79	1.63	4.04	2.83	1.21		17.17	11.68	5.49	3.62	2.82	100.01
21	2.19	22.06	38.68	0.30		12.87	6.63	4.17	2.07	-	-	-		17.32	11.23	6.09	3.64	2.95	100.01
23	2.19	21.34	30.36	-		14.07	7.25	4.60	2.22	10.31	6.98	3.33		14.03	9.19	4.84	4.32	3.48	100.01
24	2.12	20.25	30.83	-		12.77	6.62	4.45	1.70	0.26	0.19	0.07		26.68	18.85	7.83	4.19	2.90	100.00
27a	1.87	21.21	36.31	-		17.98	9.30	6.07	2.61	5.73	4.02	1.71		11.48	7.82	3.66	3.19	2.22	99.99
27b	2.65	19.56	32.91	1.01		14.09	7.30	4.86	1.92	-	-	-		23.31	16.23	6.99	3.86	2.70	99.99
28	1.18	17.62	43.09	0.70		9.18	4.78	3.32	1.08	-	-	-		23.59	17.42	6.18	3.12	1.52	100.00
30	0.47	17.31	44.67	-		8.50	4.42	3.05	1.03	3.88	2.91	0.97		21.10	15.44	5.66	2.99	1.07	99.99
31	0.97	22.66	38.28	-		11.92	6.16	4.02	1.74	1.84	1.29	0.55		19.15	13.02	6.13	3.41	1.77	100.00
32	1.65	22.34	40.49	-		12.59	6.51	4.24	1.84	0.36	0.25	0.11		17.42	11.83	5.59	3.17	1.98	100.00
33	1.39	21.50	39.48	-		12.18	6.29	4.02	1.87	10.43	7.14	3.29		10.14	6.73	3.41	3.21	1.67	100.00
35	2.96	23.79	37.26	-		10.52	5.41	3.56	1.74	4.71	3.11	1.60		14.24	9.10	5.14	3.65	2.87	100.00
36	3.24	23.55	36.74	-		10.51	5.42	3.47	1.61	2.63	1.81	0.83		17.01	11.29	5.71	3.56	2.76	100.00
37	1.13	15.69	38.27	0.56		15.07	7.85	5.43	1.80	-	-	-		22.86	16.81	6.05	3.52	2.90	100.00
42	1.73	18.57	29.89	-		21.79	11.19	6.87	3.72	10.17	6.62	3.55		10.25	6.44	3.80	4.44	3.17	100.00
43	2.16	21.91	30.78	-		14.87	7.66	4.83	2.38	8.34	5.61	2.73		15.10	9.84	5.27	4.14	2.70	100.00
48	1.16	20.83	40.74	-		10.78	5.59	3.74	1.44	2.76	2.00	0.76		18.79	13.23	5.56	3.18	1.76	100.00
49	1.26	17.71	37.38	-		13.19	6.83	4.50	1.86	4.11	2.92	1.19		20.58	14.18	6.39	3.80	1.97	100.00
50	1.33	20.06	43.60	-		8.08	4.19	2.82	1.07	4.52	3.29	1.23		17.93	12.70	5.23	3.02	1.46	100.00
52	2.07	20.42	33.05	-		12.19	6.32	4.21	1.66	1.67	1.20	0.47		24.10	16.86	7.24	3.99	2.51	100.00
53	2.49	24.26	36.81	-		13.38	6.90	4.36	2.13	5.68	3.83	1.85		11.43	7.46	3.97	3.32	2.63	100.00
54	2.68	21.78	39.16	1.51		9.11	4.72	3.13	1.26	-	-	-		20.08	13.97	6.11	3.53	2.56	100.01
56	5.16	26.94	31.70	-		15.28	7.83	4.68	2.77	2.06	1.30	0.76		12.61	7.66	4.95	3.56	2.69	100.00
CRD-24	4.31	27.65	28.89	-		13.66	7.03	4.44	2.19	2.81	1.89	0.92		16.07	10.46	5.62	3.73	2.89	100.01
CRD-29	1.81	23.69	33.37	-		9.18	4.76	3.18	1.24	0.13	0.09	0.04		25.63	17.99	7.65	3.84	2.35	100.00
NC-3	1.08	23.19	35.45	-		14.49	7.53	5.11	1.85	17.86	13.15	4.72		3.89	2.79	1.10	2.67	1.38	100.01
NC-4	1.20	22.11	44.32	-		6.00	3.12	2.14	0.74	11.85	8.84	3.01		11.28	8.20	3.07	2.44	0.81	100.01
NC-16	1.69	23.34	41.41	-		10.95	5.69	3.88	1.38	8.75	6.48	2.27		10.31	7.44	2.87	2.41	1.13	99.99
NC-17	1.01	18.71	32.35	-		6.66	3.46	2.34	0.87	16.51	12.07	4.44		19.61	13.95	5.66	3.96	1.18	99.99
CRD-18	29.70	53.11	-	3.98	0.05	5.62	2.81	1.25	1.56	-	-	-	4.68	1.19	0.50	0.68	-	1.67	100.00
CRD-20	35.59	54.91	-	-	1.61	2.15	1.05	0.35	0.74	0.56	0.18	0.38	3.18	0.88	0.27	0.61	-	1.12	100.00
CRD-22	12.42	54.32	5.92	8.83	-	12.38	6.45	4.53	1.40	-	-	-	0.06(WO)	-	-	-	3.49	2.58	100.00
NC-28a	21.51	56.67	5.42	-	-	7.44	3.90	2.88	0.65	2.08	1.70	0.38	-	0.99	0.80	0.20	3.33	2.55	99.99
NC-140	23.95	51.85	5.38	4.35	-	7.85	4.08	2.78	1.00	-	-	-	-	1.09	0.78	0.31	3.19	2.34	100.00
NC-141	27.79	44.04	-	8.84	-	10.67	5.46	3.21	2.01	-	-	-	5.38	0.68	0.40	0.28	0.11	2.48	99.99
NC-142	34.42	51.34	-	3.05	0.46	5.07	2.55	1.24	1.28	-	-	-	3.53	0.72	0.34	0.38	-	1.41	100.00

VITA

Barbara Ann Olsen was born in Bangor, Maine, on July 19, 1956. After moving to New York in 1961, she attended elementary school in Uniondale and graduated with a Regents Scholarship from Uniondale High School in 1974.

In the Fall of 1975, Miss Olsen entered the State University of New York at Stony Brook, and graduated with a B.S. in geology in 1979. In September, 1979, she accepted a graduate assistantship in the Department of Geological Sciences at The University of Tennessee, Knoxville, where she began her graduate studies. She received her Master of Science degree in geology in March, 1982.

Miss Olsen is a member of the Pacific Section AAPG, the Society of Exploration Geophysicists, and Sigma Gamma Epsilon. In December, 1981, she was employed as an Exploration Geophysicist with the Gulf Oil Exploration and Production Company in Bakersfield, California.

GEOLOGIC MAP of the CONCORD GABBRO-SYENITE COMPLEX, CABARRUS COUNTY, NORTH CAROLINA

Geology by Barbara A. Olsen, modified from White and Mundorff (1944) and Bell (1960)

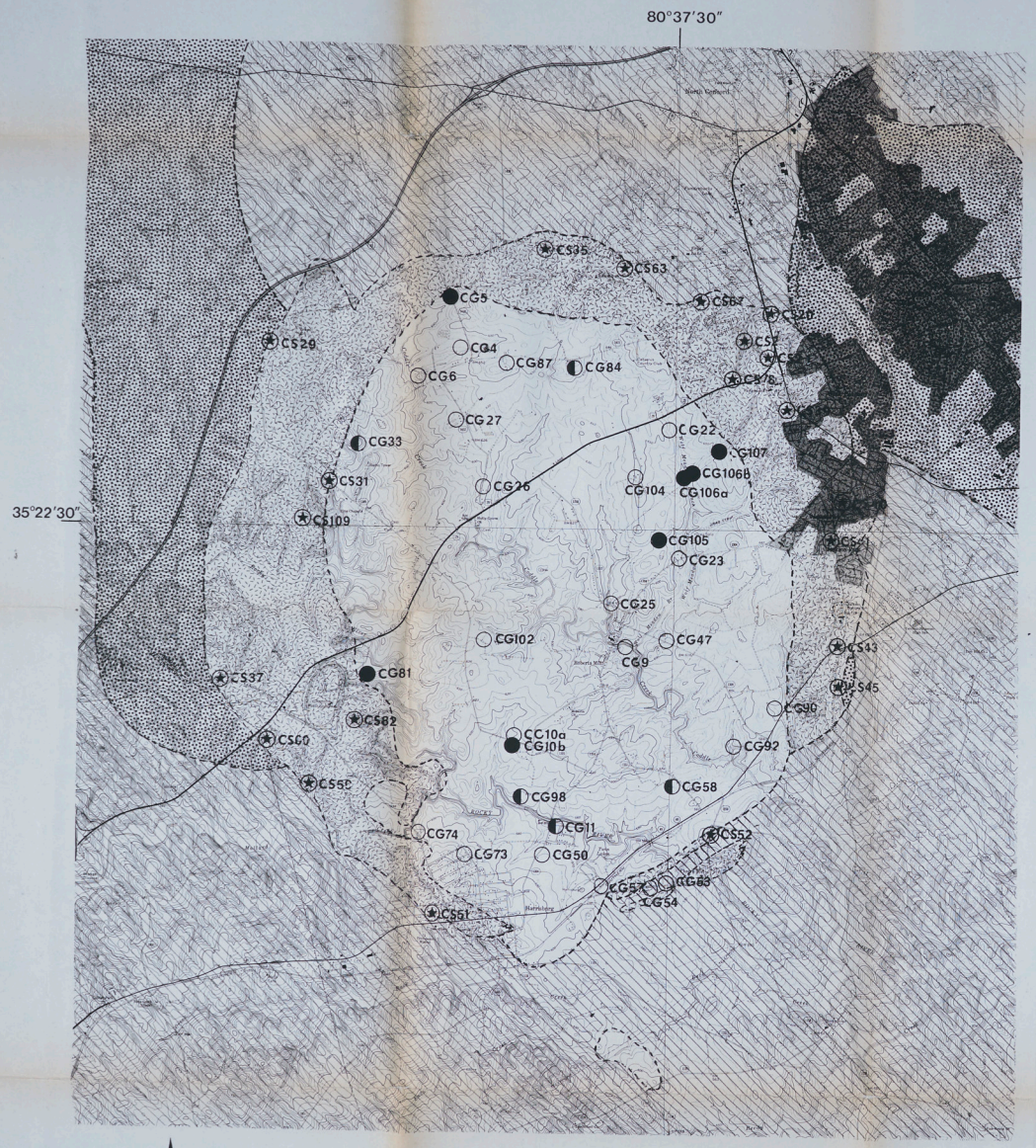

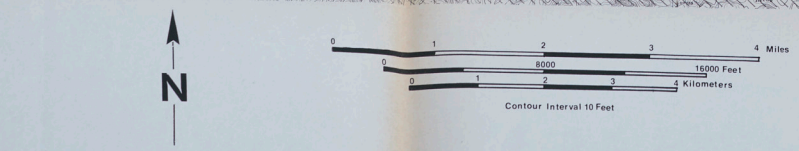

- Concord Gabbro
  - ○ OPC Sample
  - ● CPC Sample
  - ◐ OCPC Sample
- Concord Syenite
  - ⍟ Syenite Sample
- Gneissic, Granitic and Granodioritic Rocks of the Charlotte Belt
- Dioritic and Mafic Rocks of the Charlotte Belt
- Approximate Lithologic Contact

